JCI The Journal of Clinical Investigation

Splice-correcting oligonucleotides restore BTK function in X-linked agammaglobulinemia model

Burcu Bestas, … , Jesper Wengel, C.I. Edvard Smith

J Clin Invest. 2014;124(9):4067-4081. https://doi.org/10.1172/JCI76175.

Research Article **Immunology**

X-linked agammaglobulinemia (XLA) is an inherited immunodeficiency that results from mutations within the gene encoding Bruton's tyrosine kinase (BTK). Many XLA-associated mutations affect splicing of *BTK* pre-mRNA and severely impair B cell development. Here, we assessed the potential of antisense, splice-correcting oligonucleotides (SCOs) targeting mutated *BTK* transcripts for treating XLA. Both the SCO structural design and chemical properties were optimized using 2′-*O*-methyl, locked nucleic acid, or phosphorodiamidate morpholino backbones. In order to have access to an animal model of XLA, we engineered a transgenic mouse that harbors a BAC with an authentic, mutated, splice-defective human *BTK* gene. *BTK* transgenic mice were bred onto a *Btk* knockout background to avoid interference of the orthologous mouse protein. Using this model, we determined that *BTK*-specific SCOs are able to correct aberrantly spliced *BTK* in B lymphocytes, including pro–B cells. Correction of*BTK* mRNA restored expression of functional protein, as shown both by enhanced lymphocyte survival and reestablished BTK activation upon B cell receptor stimulation. Furthermore, SCO treatment corrected splicing and restored BTK expression in primary cells from patients with XLA. Together, our data demonstrate that SCOs can restore BTK function and that *BTK*-targeting SCOs have potential as personalized medicine in patients with XLA.

Splice-correcting oligonucleotides restore BTK function in X-linked agammaglobulinemia model

Burcu Bestas,[1] Pedro M.D. Moreno,[1,2] K. Emelie M. Blomberg,[1] Dara K. Mohammad,[1] Amer F. Saleh,[3] Tolga Sutlu,[4] Joel Z. Nordin,[1] Peter Guterstam,[5] Manuela O. Gustafsson,[1] Shabnam Kharazi,[4] Barbara Piątosa,[6] Thomas C. Roberts,[7,8] Mark A. Behlke,[9] Matthew J.A. Wood,[7] Michael J. Gait,[3] Karin E. Lundin,[1] Samir El Andaloussi,[1,7] Robert Månsson,[4] Anna Berglöf,[1] Jesper Wengel,[10] and C.I. Edvard Smith[1]

[1]Department of Laboratory Medicine, Clinical Research Center, Karolinska Institutet, Karolinska University Hospital Huddinge, Stockholm, Sweden. [2]Instituto de Engenharia Biomédica, Universidade do Porto, Porto, Portugal. [3]Medical Research Council, Laboratory of Molecular Biology, Cambridge, United Kingdom. [4]Department of Laboratory Medicine, Center for Hematology and Regenerative Medicine, Karolinska Institutet, Karolinska University Hospital Huddinge, Stockholm, Sweden. [5]Department of Neurochemistry, Stockholm University, Stockholm, Sweden. [6]Histocompatibility Laboratory, Children's Memorial Health Institute, Warsaw, Poland. [7]Department of Physiology, Anatomy and Genetics, University of Oxford, Oxford, United Kingdom. [8]Department of Molecular and Experimental Medicine, The Scripps Research Institute, La Jolla, California, USA. [9]Integrated DNA Technologies (IDT), Coralville, Iowa, USA. [10]Nucleic Acid Centre, Department of Physics, Chemistry and Pharmacy, University of Southern Denmark, Odense, Denmark.

X-linked agammaglobulinemia (XLA) is an inherited immunodeficiency that results from mutations within the gene encoding Bruton's tyrosine kinase (BTK). Many XLA-associated mutations affect splicing of *BTK* pre-mRNA and severely impair B cell development. Here, we assessed the potential of antisense, splice-correcting oligonucleotides (SCOs) targeting mutated *BTK* transcripts for treating XLA. Both the SCO structural design and chemical properties were optimized using 2′-*O*-methyl, locked nucleic acid, or phosphorodiamidate morpholino backbones. In order to have access to an animal model of XLA, we engineered a transgenic mouse that harbors a BAC with an authentic, mutated, splice-defective human *BTK* gene. *BTK* transgenic mice were bred onto a *Btk* knockout background to avoid interference of the orthologous mouse protein. Using this model, we determined that *BTK*-specific SCOs are able to correct aberrantly spliced *BTK* in B lymphocytes, including pro–B cells. Correction of *BTK* mRNA restored expression of functional protein, as shown both by enhanced lymphocyte survival and reestablished BTK activation upon B cell receptor stimulation. Furthermore, SCO treatment corrected splicing and restored BTK expression in primary cells from patients with XLA. Together, our data demonstrate that SCOs can restore BTK function and that *BTK*-targeting SCOs have potential as personalized medicine in patients with XLA.

Introduction

X-linked agammaglobulinemia (XLA) is the most common form of inherited agammaglobulinemia, accounting for 85% of all cases (1, 2). In this disease, a B cell lineage developmental block, manifested at the transition between the pro–B and pre–B cell stages (3), leads to the essential lack of mature B and plasma cells, with a concomitant pronounced reduction of immunoglobulin levels. XLA is caused by defects in the gene encoding Bruton's tyrosine kinase (BTK) (4–6). BTK is a cytoplasmic, nonreceptor tyrosine kinase belonging to the TEC family of tyrosine kinases (7) and is expressed in all stages of B cell development, with the exception of long-lived, antibody-producing plasma cells (8, 9). Besides B lymphocytes, many other hematopoietic cells also express BTK (5, 8–10), but clinically relevant functional impairment seems to be confined to this lineage. Thus, the severe clinical outcome of *BTK* mutations demonstrates the essential role of BTK already occurring in pre–B cell receptor signaling, which is a determinant for proliferation, differentiation, and survival of the early B cell stages (3, 11, 12).

Patients with XLA are prone to recurrent infections by pyogenic bacteria, such as pneumococci and streptococci. Affected subjects are also unduly susceptible to enteroviruses, which cause dermatomyositis and fatal chronic encephalomyelitis (13–16). The current treatment for XLA consists of prophylactic, regular intravenous, or subcutaneous gammaglobulin replacement therapy and generous administration of antibiotics. This considerably improves quality of life, but patients still suffer from chronic infections (17, 18). Furthermore, life expectancy is reduced despite appropriate care (16, 19–21).

Splicing defects have been identified as an important cause of genetic disease. Many mutations affecting splicing disrupt the regular 5′ splice site (5′ss) or 3′ss at exon-intron junctions. Further, mutations can create new splice sites, which may result in the inclusion of intronic sequences or loss of part of the exons in the transcript. When such a new splice site occurs in an intron in the vicinity of a suitable pseudo splice site, the intervening intronic region can be included in the mRNA as a cryptic exon. This mechanism has been observed in multiple diseases, including cystic fibrosis (22) and ataxia telangiectasia (23, 24) among others. In XLA, we have previously identified and described 2 such families (25, 26).

Authorship note: Burcu Bestas and Pedro M.D. Moreno contributed equally to this work.
Conflict of interest: Patent applications have been filed relating to the technologies described herein, which are assigned to IDT. Mark A. Behlke is employed by IDT but does not personally own any shares or equity in IDT. IDT is not a publicly traded company.
Submitted: March 21, 2014; **Accepted:** July 3, 2014.
Reference information: *J Clin Invest*. 2014;124(9):4067–4081. doi:10.1172/JCI76175.

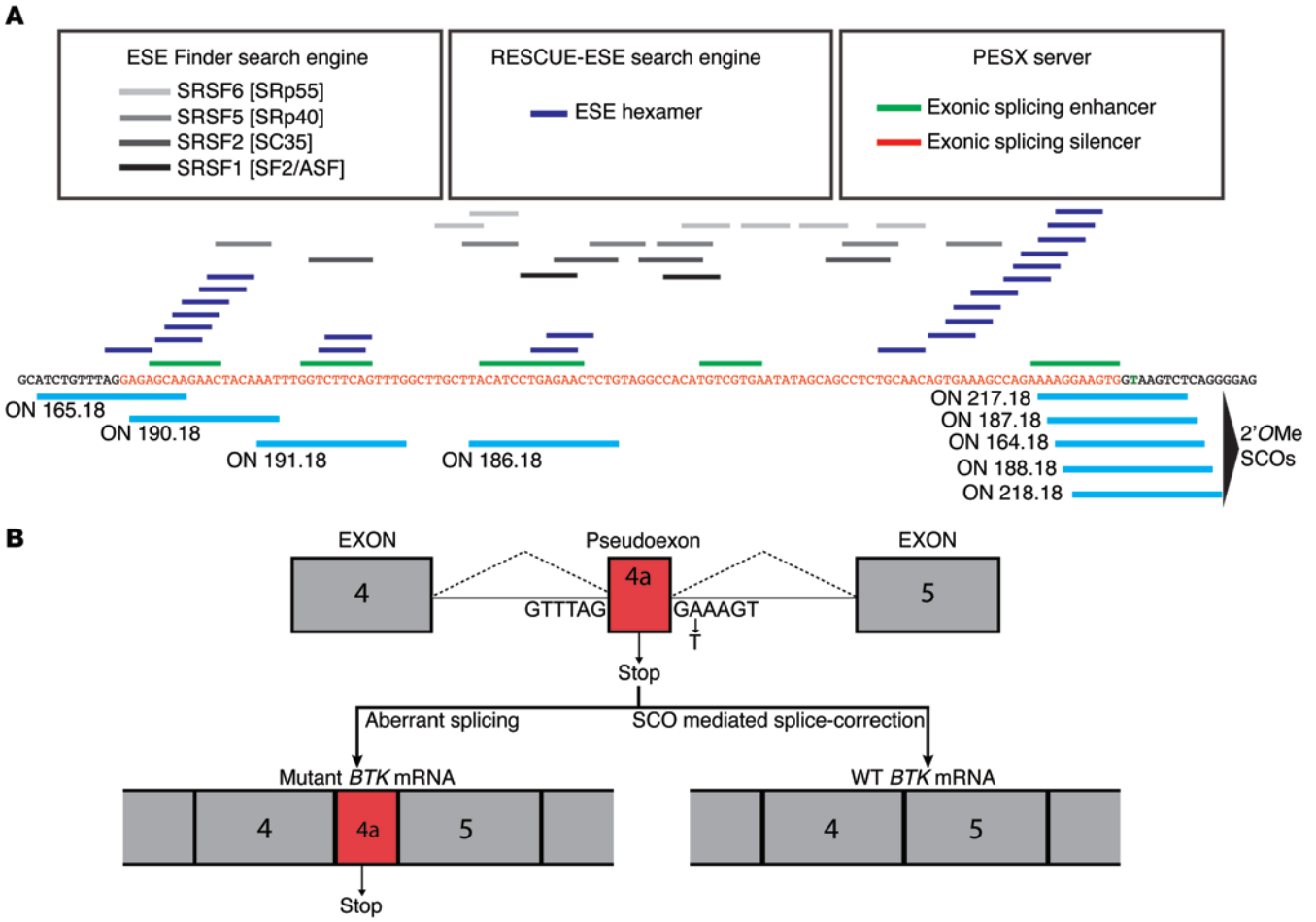

Figure 1. Design of SCOs using bioinformatic tools to search for ESE sites in the disease-causing pseudoexon. (**A**) Three different algorithms from the corresponding web-based servers, ESE-Finder, RESCUE-ESE, and PESX, were used, and the hits were aligned to the pseudoexon sequence to find locations with the highest correlation between algorithms. SCOs targeting the probable ESE regions were subsequently designed. SCOs are schematically presented with their binding-positions along the pseudoexon. (**B**) Predicted outcome of splicing, with or without SCOs, indicated schematically.

The XLA defect studied in this work arises from one of these families, which has an A-to-T transition in intron 4 of the *BTK* gene generating a novel 5′ss. This, together with a preexisting cryptic 3′ss upstream in the same intron, results in the inclusion of a cryptic exon (exon 4a) of 109 nucleotides between exons 4 and 5 in the mRNA (25). This changes the reading frame and completely abolishes BTK protein expression. The erroneous inclusion of exon 4a prompted us to investigate the possibility of using splice-correcting antisense oligonucleotides (SCOs), which bind to and restore the splicing of the pre-mRNA, a concept also exploited in other diseases, as reviewed recently (27, 28).

Apart from the splice sites themselves, splicing is also controlled by short regulatory sequence motifs in both exons and introns. These motifs are designated exonic or intronic splicing enhancers (ESEs or ISEs, respectively) or exonic or intronic splicing silencers (29). These are also of interest since SCOs targeting exonic splicing silencers have been shown to induce the inclusion of exon 7 in the transcript of the *SMN2* gene in spinal muscular atrophy (30). Similarly, exonic splicing silencer regions have been targeted in the case of Duchenne muscular dystrophy (DMD), which is caused by mutations in the *DMD* gene. In this case, restoration of a disrupted reading frame by exon-skipping SCOs has been used successfully to generate a truncated but partially functional protein (31, 32).

Here, we describe the feasibility of splice correction by preventing cryptic exon inclusion as a personalized therapy for XLA. In order to achieve this, we designed SCOs targeting various sites in the pseudoexon region of *BTK* pre-mRNA. Different oligonucleotide (ON) chemistries have been developed over recent years in order to improve resistance to degradation, enhance target affinity, and promote cellular uptake. In this study, we investigated SCOs with 2′-*O*-methyl phosphorothioate (2′OMePS) or phosphorodiamidate morpholino (PMO) backbone chemistries. For simplicity, the splice-correcting PMO-based oligomers are also referred to as SCOs.

The PMO was also tested in a cell-penetrating peptide–conjugated (CPP-conjugated) version. CPPs are a class of peptides with the ability to translocate rapidly into cells and to transport various macromolecular cargos. PMO-based SCOs conjugated with CPPs have been shown to be very efficient as therapeutics against splice abnormalities, especially in the *mdx* mouse model of DMD (33). Furthermore, we investigated nucleic acid modifications, such as locked nucleic acid (LNA), since they have been used successfully in many different settings, such as antisense gapmers, siRNAs,

Table 1. SCOs used in the study

ON (SCO)	Sequence (5′→3′)
2′-*O*-methyl RNA	–
164.18	ugagacuuaccaccuccu
165.18	uugcucuccuaaacagau
186.18	cagaguucucaggaugua
187.18	gagacuuaccacuuccuu
188.18	cugagacuuaggacuucc
190.18	auuuguaguucuugcucu
191.18	caaacugaagaccaaauu
217.18	agacuuaccacuuccuuu
218.18	ccugagacuuaccacuuc
705.18 (unrelated control)	ccucuuaccucaguuaca
LNA/2′-*O*-methyl RNA and DNA	–
190.15-5LNA	uTugTagTucTugCu
187.15-5LNA	aGacTuaCcaCuuCc
187.18-6LNA	gAgaCuuAccAcuTccT
187.12-8LNA	AcTTaCCaCTTc
187.12-8LNA-4LNAgly	AcXXaCCaCXXc
187.10-9LNA	TTACCaCTTC
186.15-3LNA	gAguucuCaggauGu
186-15-5LNA	gAguTcuCagGauGu
186.15-6LNA-2UNA	gAgTucuCaGgaTGu
186.15-3LNA-2UNA	gAguucuCaggauGu
186.12-8LNA-3LNAgly	TX**c**XCA**gg**AX**g**T
186.12-8LNA-4LNAgly	TX**c**XCA**gg**AX**g**X
186.12-8LNA-5LNAgly	XX**c**XCA**gg**AX**g**X
186.12-8LNA	TTcTCAggATgT
5′186.12-7LNA	AgTTcTCagGaT
GAA.12-6LNA	cTaTaTTCaCga
GAA.19-3LNA	cuTccuuuTcuggcuuTca
GAA.19-6LNA	cuTccTuuTcuGgcTuuCa
Scrambled	cAcuCuaTauAacTg
ZEN LNA/2′-*O*-methyl RNA	–
186.15-5LNA-ZEN	g/ZEN/AguTcuCagGauG/ZEN/u
186.18-ZEN	c/ZEN/agaguucucaggaugu/ZEN/a
PMO & B-PMO	–
B-PMO 186.25	B-peptide-CTACAGAGTTCTCAGGATGTAAGCA
Scrambled B-PMO (DMD)	B-peptide-GGCCAAACCTCGGCTTACCTGAAATT
B-peptide	N-RXRRBRRXRRBRXB-C

B-peptide was conjugated to PMO 186.25 to generate B-PMO 186.25. 2′-*O*-methyl RNA SCOs (including those modified by LNA and ZEN) have phosphorothioate backbone. LNA bases are in uppercase letters; 2′-*O*-methyl RNA bases are in lowercase letters; UNA bases are underlined; DNA bases are in bold letters; "X" represents amino-glycyl-LNA-T.

anti-microRNAs (antagomirs), and anti-gene approaches (34, 35). An LNA-containing ON with its 3′-endo conformation is considered to be an RNA mimic, making it effective toward structured RNA regions, which can be beneficial when targeting pre-mRNAs. This is due to the fact that position-dependent substitution with LNA bases changes the thermodynamic property of the duplexes (34, 36). Additionally, we also investigated LNA in combination with other derivatives, such as unlocked nucleic acid (UNA) or amino-glycyl-LNA (34). Moreover, since the nonbase modifier *N*,*N*-diethyl-4-(4-nitronaphthalen-1-ylazo)-phenylamine (ZEN) has been shown recently to have potentiating effect for antagomirs, it was also tested (37).

We targeted primary patient cells as well as lymphocytes from a genetically altered mouse created for this purpose. This transgenic mouse has several unique features; it carries the entire human mutant *BTK* locus and is devoid of endogenously expressed BTK protein. Notably, in contrast to the treatment concept for DMD, in which a truncated protein with reduced function is formed, the strategy in XLA permits the restoration of the authentic reading frame generating a fully functional protein. Importantly, because of the developmentally regulated expression of BTK, it may become feasible to achieve long-term correction of the disease phenotype. Moreover, besides proving the viability of splice-modifying therapy for a novel target disease both ex vivo and in vivo, we demonstrate for the first time that both primary B cells and primary monocytes are amenable to splice correction strategies.

Results

Design of SCOs using bioinformatics tools. Different SCOs directed against the *BTK* pseudoexon region were designed, taking into consideration not only the 3′ss and 5′ss of exon 4a, but also putative ESE sites. For this purpose, we used 3 different algorithms from the web-based servers ESE Finder, PESX, and RESCUE-ESE. The sequence hits were aligned to exon 4a, as depicted in Figure 1, which also shows the studied mutation and the expected outcomes with or without splice correction. This analysis prompted us to generate a set of SCOs, as schematically indicated in Figure 1. They were designed to cover the 3′ss and 5′ss and the ESEs sites that demonstrated the most concordance between the algorithms used. The first set of SCOs was composed of the commonly used 2′OMePS modification, taking into consideration the GC content, self-dimerization, and nucleic acid melting temperature (*T*m) values (38). Additional sets were then designed with various modifications and lengths. A schematic representation of the SCOs is shown in more detail in Supplemental Figure 1 (supplemental material available online with this article; doi:10.1172/JCI76175DS1), and the modifications are indicated in Table 1.

SCOs restore luciferase mRNA in a reporter cell line model. We first designed a reporter construct containing the expression cassette for a fusion of EGFP and firefly luciferase but interrupted by the mutated patient-derived *BTK* intron 4. When uncorrected, this minigene produces a corrupt EGFP-luciferase mRNA. However, introduction of an SCO capable of rescuing the splicing of the mutated intron would promote restoration of EGFP-luciferase fusion protein expression. The model was constructed as a first functional readout for SCO activity and used to generate a stable U2OS reporter cell line expressing the above-mentioned corrupt transcript. Subsequently, the fully 2′OMePS-modified SCOs (sequences depicted in Table 1) were transfected, and luciferase enzymatic activity was determined (Figure 2A). Several of the tested SCOs showed promising results when compared with the unrelated, control SCO 705 directed against a mutated β-globin intron (39). SCO 187, covering the 5′ss, performed the best in these experiments, whereas SCO 165, covering the 3′ss, demonstrated very low efficacy. SCOs 186, 187, and 190 were chosen for further experiments. SCOs 186 and 190 were selected because of their activity and the fact that they were not targeted to splice sites but instead to the predicted ESEs.

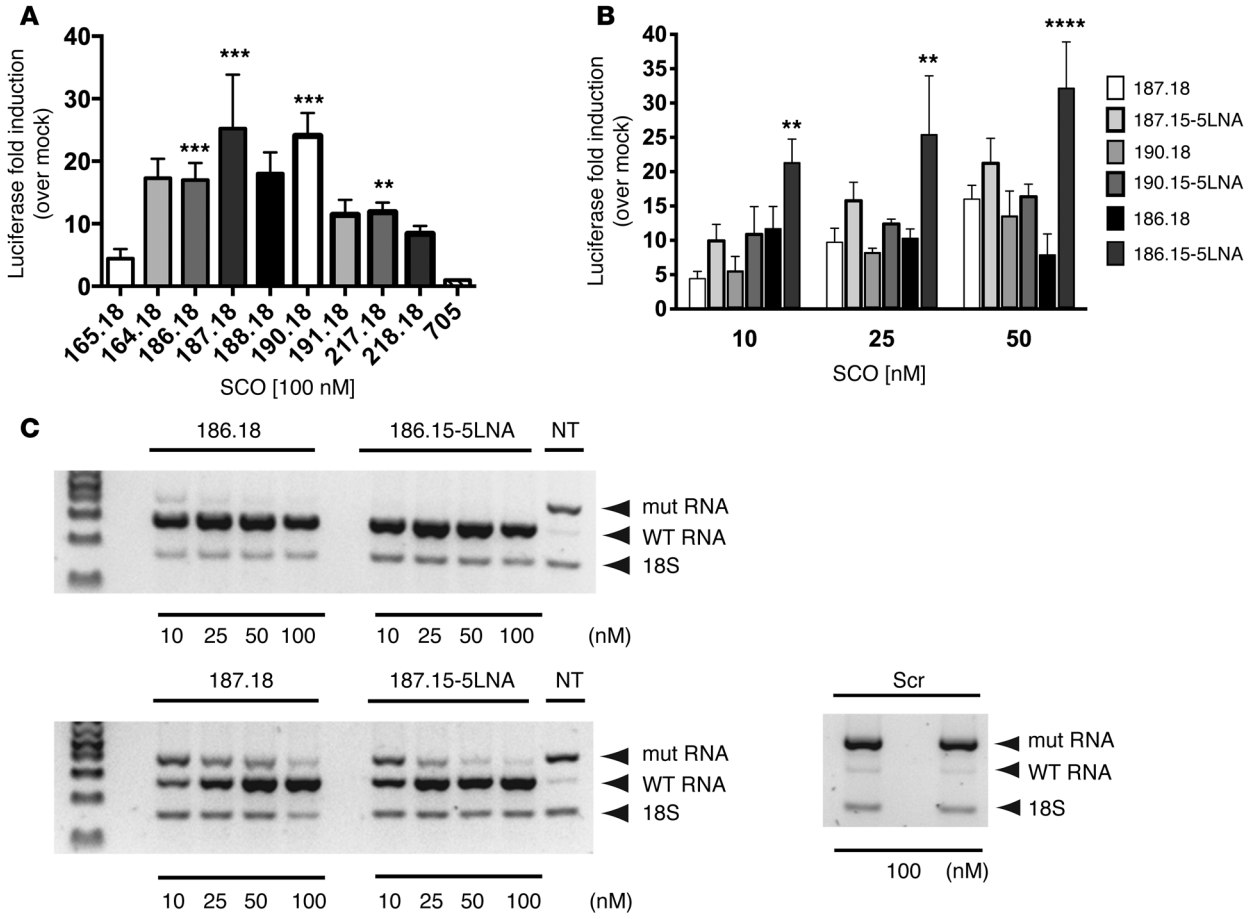

Figure 2. Splice correction–induced upregulation of reporter minigene activity. The U2OS cell line stably carrying a minigene interrupted by the mutated *BTK* intron 4 was transfected with different SCOs, and efficacy was measured as luciferase activity or mRNA restoration. (**A**) The relative luciferase activity in comparison to nontreated cells (mock) 24 hours after SCO transfection. "705" indicates an unrelated control SCO, targeting position 705 of a mutated β-globin intron, not complementary to the *BTK* pre-mRNA. All tested SCOs are 2′OMePS based (Table 1). Data represent mean + SD of 3 independent experiments, each with 2 replicates. $^{**}P \leq 0.01$, $^{***}P \leq 0.001$, versus 705. (**B**) Increase in luciferase activity by 2′OMePS-modified SCOs versus LNA SCOs is presented as fold increase over nontreated cells (mock). Graph represents mean + SD of 3 independent experiments, each with 2 replicates. $^{**}P \leq 0.01$, $^{****}P \leq 0.0001$, 186.18 versus 186.15-5LNA. (**C**) Total RNA RT-PCR showing the 389-bp and 271-bp bands corresponding to aberrant and corrected (with *BTK* intron 4 excised) mRNA bands, respectively, with a lower band of ribosomal RNA (18S) serving as an RNA quality control. The lane on the right represents RNA input from nontreated (NT) cells. "Scr" represents the control LNA/2′OMePS SCO not complementary to the reporter gene sequence (Table 1). A representative gel from 2 independent experiments is shown. Statistical significance was determined using 1-way ANOVA, followed by Bonferroni's multiple-comparison test.

SCO chemistry affects splice correction activity in reporter cell line. We modified the selected SCOs with LNA bases, which are known to significantly enhance *T*m and increase the efficiency of ONs both in vitro and in vivo (40–44). More specifically, we chose a 2′OMe RNA backbone with LNA modifications, as this combination has previously demonstrated high potency (45–48). Since size-reduced SCOs are generally considered to be more efficient (34, 42, 49), with lowered risk of off-target effects and improved uptake, we designed LNA-modified 15-mer versions of the 186, 187, and 190 series (Supplemental Figure 1 and Table 1). Figure 2 shows the activity of LNA-modified SCOs in the U2OS reporter cell line, as measured by luciferase expression and as also confirmed by the correction of mRNA determined by RT-PCR. It is clearly shown that the LNA-modified SCOs mediate enhanced luciferase activity at low concentrations. The same tendency was confirmed at the RNA level, at which we observed a reduction of the aberrant mRNA band and a concomitant appearance of the corrected form at low SCO concentrations. The 190 series of SCOs was not further assessed, since at higher concentrations there were signs of toxicity in the form of cell death 24 hours after transfection (data not shown).

Based on these results we further modified the 186 and 187 series, including a reduction of the ON length further to 10 to 12 nucleotides. We also synthesized 3 additional SCOs, referred to as the GAA series. These were designed to target GAA-triplets, known to be present in certain splicing-enhancers (26, 50), as shown in Supplemental Figure 1 and Table 1. Supplemental Figure 2 depicts the effect of SCOs derived from the 186, 187, and GAA series, as analyzed by RT-PCR. The doses were lowered, as compared with previous experiments (Figure 2), in order to identify the most potent SCOs. As can be seen in Supplemental Figure 2, LNA-modified SCOs displayed higher potency as compared with their corresponding 2′OMePS versions. 186.15-5LNA and 186.15-3LNA (with 5 and 3 LNA substitutions, respectively) showed the best efficiency

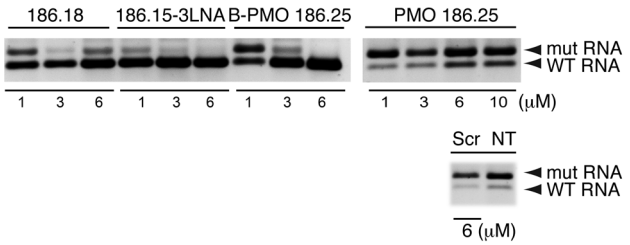

Figure 3. Splice correction–induced upregulation of reporter minigene activity following naked uptake of SCOs. SCOs from the 186 series, including PMO 186.25, with and without the CPP moiety (B-PMO 186.25), were tested, and activity was measured as restoration of mRNA. A concentration of 6 μM was used for the scrambled control SCO (Scr) (Table 1). A representative gel from 2 independent experiments is shown.

in the reporter cell assay. The 12-mer versions of both the 186 and 187 series did not exhibit any enhanced activity under these in vitro conditions, and the 10-mer of SCO 187 was inactive (Supplemental Figures 2 and 3). Moreover, the newly designed GAA series did not show better efficiency compared with 186.15-5LNA or 186.15-3LNA and was therefore not studied further.

In addition, we investigated 3 more chemical modifications (Table 1): amino-glycyl-LNA, UNA, and the nonbase modifier ZEN. The amino-glycyl modification adds a glycyl residue to the N2′ position of 2′-amino-LNA, thereby providing a positive charge (51). UNA is known to decrease the *T*m and destabilize the duplex, which potentially could increase target specificity if appropriately designed (52). ZEN is a naphthyl-azo modifier; when placed at or near both ends of a 2′OMe ON, it increases *T*m and enhances the stability against endo- and exonucleases (37). These new modifications were also tested in the reporter cell line model. As can be seen in Supplemental Figure 3, the glycyl-modified 12-mer versions of 186 and 187 series showed reduced activity with increasing numbers of amino-glycyls correlating to further reduction in activity. This was somewhat unexpected, since the reduced net negative charge potentially could have enhanced their splice-correcting capacity by allowing better hybridization to the cognate pre-mRNA. On the other hand, decreased net negative charge might also have reduced the complexation with the transfection reagent Lipofectamine 2000, which potentially could have altered both the complex conformation and the amount transfected into cells. Conversely, UNA incorporation into the 186 series of SCOs caused reduced activity at low LNA content, whereas with higher LNA content the activity was somewhat restored. Moreover, ZEN-modified SCO (186.15-5LNA-Zen), as compared with 186.15-5LNA (Supplemental Figure 2), did not show much difference in activity. The slightly longer 186.18-ZEN had almost the same effect as 186.15-5LNA and 186.15-3LNA. This might suggest that ZEN modification is more useful when used in the context of a pure 2′OMe backbone and not when combined with shorter LNA ONs. Taken together, these additional modifications did not show enhanced activity and were not studied further.

LNA-based SCOs and PMOs conjugated to a CPP are efficiently taken up (gymnosis) in the reporter cell line. We next investigated the naked uptake efficiency in the reporter cell line under "gymnosis" conditions. The term gymnosis was coined by Stein et al. to describe uptake of LNA gapmers by cells in the absence of any transfection reagent (53). The authors suggested that this mode of in vitro delivery better correlated to in vivo uptake, making this method of general interest. Compared with lipofection, considerably higher concentrations of ONs are needed for gymnosis.

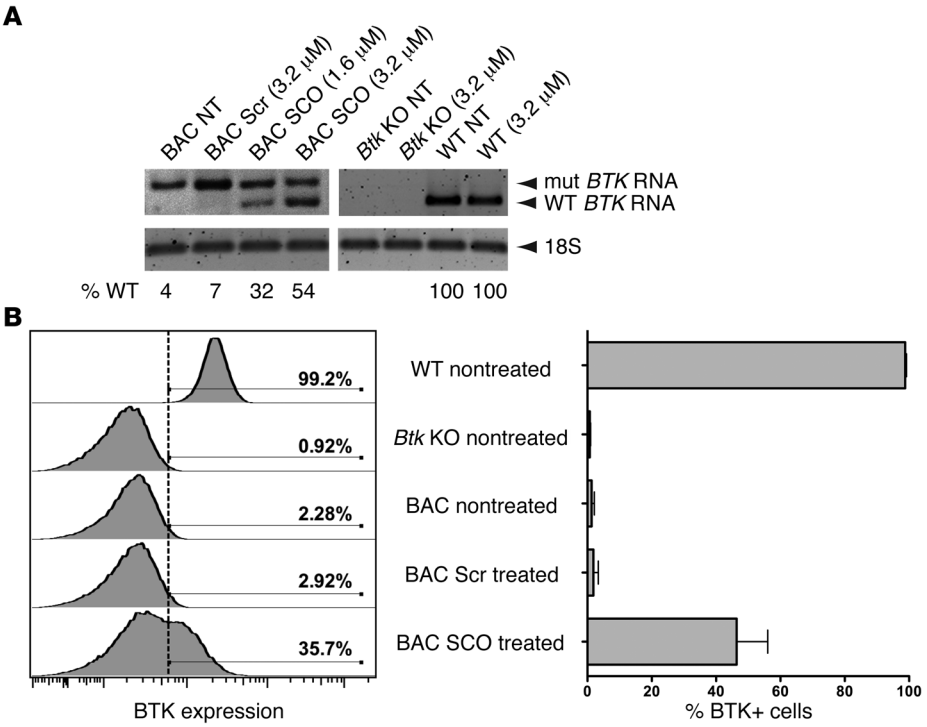

Figure 4. Full-length human mutated *BTK* pre-mRNA corrected by SCOs yielding normal-sized transcripts and detectable BTK protein. (**A**) B cells from human BAC transgenic mice were treated with 1.6 μM or 3.2 μM 186.15-3LNA SCO and analyzed by RT-PCR. To identify human RNA in cells from BAC transgenic and KO mice, a primer pair only detecting human *BTK* was used. To measure endogenous mouse *Btk* mRNA levels in splenocytes derived from WT mice, a different primer set selective for mouse *Btk* was used. A representative gel from 3 independent experiments is shown. Ribosomal RNA (18S) was used as an RNA quality control. (**B**) FACS analysis of cells 48 hours after treatment with 186.15-3LNA. B cells were stained with antibodies directed against CD19 or BTK protein (recognizing both mouse and human protein). Histograms for BTK expression in each sample from a representative experiment as well as the percentage of corrected cells from 3 independent experiments are shown (mean + SD). A concentration of 3.2 μM was used for the scrambled control SCO (Table 1). Mean fluorescence intensity, WT NT: 2,314; BAC SCO treated: 1,210. Percentage of WT *BTK* RNA was calculated as WT RNA fraction × 100/(misspliced + WT RNA fractions).

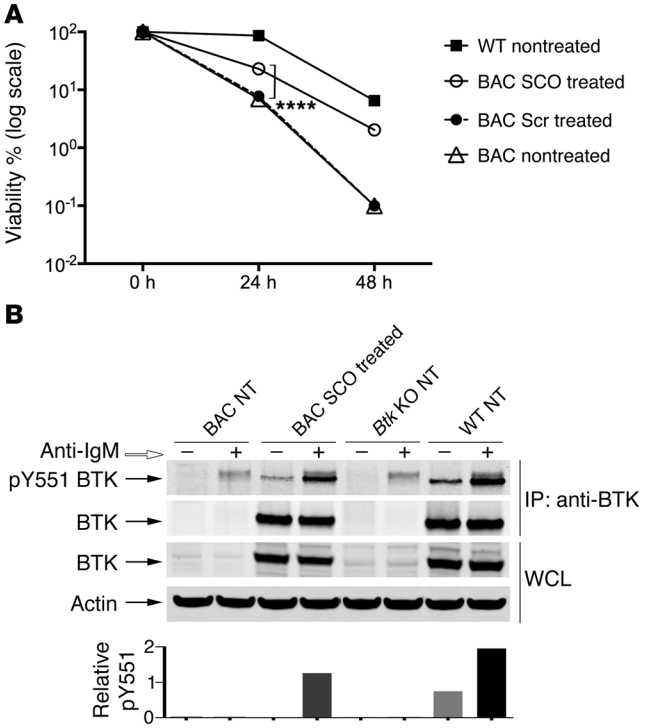

Figure 5. Enhanced survival and anti-IgM–induced BTK tyrosine phosphorylation in SCO-treated BAC transgenic B cells. (**A**) Spleen B cells from BAC transgenic mice were treated with 3.2 μM SCO (186.15-3LNA or scrambled control) and stimulated with 20 μg/ml anti-IgM 48 hours after electroporation (time 0). Cells were counted, and viability was determined by trypan blue exclusion 24 and 48 hours after stimulation. The initial number of cells from both WT and BAC transgenic mice was 2×10^6. Data represent 2 independent experiments with duplicates. Note that nontreated and scrambled ON–treated cell numbers overlap. Statistical significance was analyzed by using 1-way ANOVA followed by Bonferroni's multiple-comparison test. ****$P \leq 0.0001$ for BAC SCO treated versus BAC Scr and NT at 24 hours. (**B**) Analysis of BTK tyrosine phosphorylation after 3.2 μM SCO (186.15-3LNA) treatment and anti-IgM stimulation (20 μg/ml). Blots show pY551 phosphorylation of BTK and total BTK. Whole cell lysate (WCL) analysis shows BTK protein and actin. Each duplicate (–/+) corresponds to starved or anti-IgM–activated conditions. A representative blot is shown from 2 independent experiments. Note that the higher molecular weight band, located immediately above the pY551-BTK band in activated samples (IP pY551 gel), is of unknown origin and unrelated to BTK, since it also exists in B cells obtained from *Btk* KO mice following stimulation. The bar graph shows the quantitative analysis of Y551 phosphorylation as a percentage of relative intensity signal from the blots according to ImageJ Software.

We selected the most efficient SCOs based on the results from the lipofection experiments and assessed their gymnotic activity. Although 186.15-5LNA exhibited good activity, we continued with the similarly efficient 186.15-3LNA, owing to the fact that reduced LNA content potentially could reduce off-target effects (45). Although ZEN-modified SCOs had similar activity compared with the LNA-containing 186.15 versions, they could not be studied, since their availability was limited.

In addition, we also investigated the PMO backbone (54, 55), with the 186 sequence in the gymnosis setting. Owing to the rules of PMO design, this SCO was further extended to be 25 nucleotides (Supplemental Figure 1 and Table 1). The rationale for lengthening PMOs is the lower target affinity (56). We further conjugated the PMO with a CPP moiety named B-peptide (B-PMO), since it is known to be very active for exon skipping in the *mdx* mouse model (57). Thus, the PMOs tested were either unmodified or covalently conjugated to B-peptide.

As can be seen from Figure 3, in gymnosis setting, 186.15-3LNA and B-peptide–conjugated PMO 186.25 (B-PMO) showed high potency in the reporter cells when analyzed by RT-PCR. We also tested higher (up to 10 μM) concentrations of PMO 186.25, which were devoid of any CPP; however, the exon-skipping effect was very low.

Generation of a transgenic mouse carrying the mutated human BTK locus. In order to have access to an unlimited supply of mutated B-lineage cells as well as a relevant in vivo model, we generated a mouse carrying the corresponding human *BTK* locus. A suitable BAC clone named RP11-125I5 was chosen for the development of BAC transgenic mice. This clone encompasses 175 kb and contains an extended human genomic *BTK* locus. The BAC was subsequently subjected to site-specific mutagenesis, generating a single-point mutation at position 602 of *BTK* intron 4, the very same A-to-T change as seen in the XLA-family described previously. We confirmed that the BAC transgenic mice carry the mutated human *BTK* gene by sequencing of chromosomal DNA (data not shown). The founder animals were then backcrossed onto *Btk* knockout (KO) mice in order to generate transgenic animals with a disrupted, nonfunctional endogenous *Btk* locus, which were therefore only capable of expressing the mutated human *BTK* gene (Supplemental Figure 4). Throughout this report we refer to these mice as BAC transgenic mice. We also verified that the insertion of the transgene did not influence hematopoietic development; Supplemental Figure 5 shows that the common lymphoid progenitors and B cell compartment are similar in *Btk* KO and BAC transgenic mice.

SCOs correct mRNA and restore BTK protein in primary B cells ex vivo. To test the activity of the SCOs in the context of a full-length pre-mRNA transcribed from the mutant human *BTK* gene, we isolated splenic B cells from mice expressing the human mutant *BTK* transcript. As control, we used B cells from WT and *Btk* KO mice. For transfections of SCOs, we optimized a protocol for electroporation of mouse primary B cells. At 48 hours after electroporation, cells were collected, and human *BTK* RNA was analyzed by semiquantitative RT-PCR, using primers detecting only human *BTK*. Another primer set was used to specifically amplify mouse *Btk* RNA in order to verify that this transcript is unaffected by the SCOs (Figure 4A). The results clearly show that, by using SCO 186.15-3LNA, splicing of the full-length human mutant *BTK* pre-mRNA was corrected, as demonstrated by the appearance of a lower molecular weight amplicon corresponding to the size of unmutated, native *BTK* mRNA. The correction was also verified by sequencing the cDNA (data not shown).

The RT-PCR results were also confirmed by flow cytometry analysis on cells collected 48 hours after transfection (Figure 4B). As can be seen from Figure 4B, treatment with 186.15-3LNA gen-

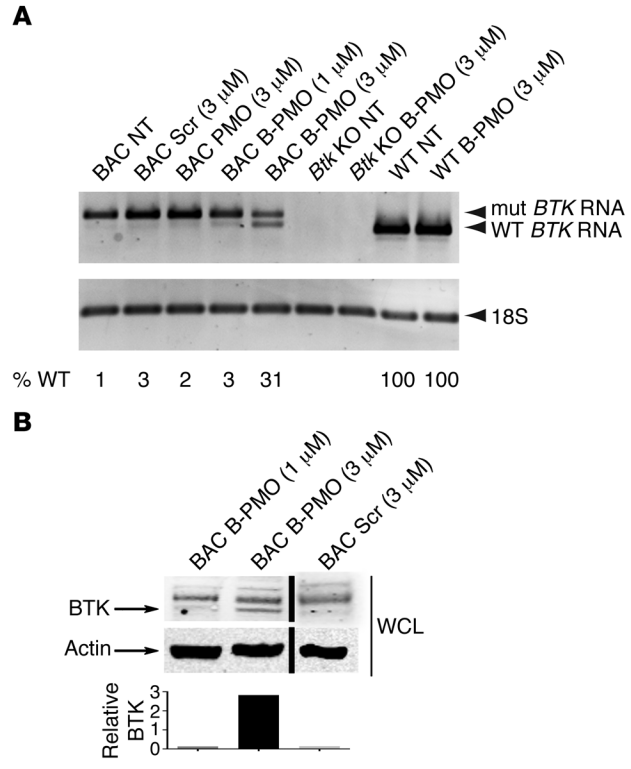

Figure 6. B-PMO–mediated restoration of *BTK* mRNA and protein in primary spleen B cells from human BAC transgenic mice. Cells were treated with PMO 186.25 or B-PMO 186.25 in different concentrations. "Scr" indicates a B-PMO SCO for an unrelated target (DMD). (**A**) RT-PCR products from SCO-treated B cells at 1 and 3 μM concentrations. Ribosomal RNA (18S) serves as an RNA quality control. Of note, for the splenocytes derived from WT mice, a different primer set selective for mouse *Btk* was used. The percentage of WT *BTK* RNA was calculated as WT RNA fraction × 100/(misspliced + WT RNA fraction). (**B**) Western blot from the same treatment. Experiments were repeated 3 times, and representative gels are depicted. Of note, for this experiment, anti-BTK from BD (see Methods) was used, yielding different unspecific bands. The bottom band originates from BTK, while the top band is unspecific. The lanes separated by a black line were run on the same gel, but since some lanes were considered uninformative, they were omitted as indicated by the black line. The bar graph shows the quantitative analysis of BTK protein as a percentage of relative intensity signal according to ImageJ Software. Scr, treated with scrambled ON.

erated a mean of over 40% of cells expressing substantial levels of BTK protein. These experiments demonstrate that not only the reporter minigene-derived transcript carrying the mutated *BTK* intron, but also the full-length human *BTK* pre-mRNA is amenable to SCO therapy.

SCOs restore functional BTK in primary B cells from the BAC transgenic mouse. Since we could conclusively show the presence of BTK protein by flow cytometry analysis, we investigated whether the synthesized protein is also functionally active. For this purpose, 2 functional assays were carried out, cell viability and phosphorylation of the BTK regulatory loop tyrosine (Y551).

The rationale for the cell viability test is that impaired maturation and survival of B cells are hallmarks of XLA (1, 2, 13). Moreover, it is known that BTK-deficient mouse B cells do not proliferate in response to anti-IgM stimulation, while WT cells do (58, 59). Therefore, we stimulated BAC transgenic mouse B cells 48 hours after SCO treatment with anti-IgM and incubated them for another 24 or 48 hours in the absence of the survival-promoting CpG stimulus (see Methods), conditions rather harsh for primary B cells. Figure 5A shows the viability of primary B cells after 24 or 48 hours of incubation with anti-IgM. As seen, under these experimental conditions SCO-treated BAC transgenic B cells showed enhanced survival compared with nontreated or scrambled, SCO-treated cells. As a sign of the harsh environment, WT mouse B cells were also reduced in numbers. As a second proof of BTK functionality, we analyzed the BTK phosphorylation after B cell receptor stimulation. In normal B cells, upon anti-IgM treatment, B cell receptor–induced signaling leads to tyrosine Y551 phosphorylation of BTK. The corresponding tyrosine is conserved in all cytoplasmic protein-tyrosine kinases and upon phosphorylation significantly enhances their catalytic activity owing to a conformational change (3, 13). SCO-treated B cells from BAC transgenic mice were compared with B cells from WT mice. 48 hours after electroporation, cells were serum starved for 6 hours and subsequently incubated with 20 μg/ml anti-IgM before harvest. BAC transgenic B cells treated with 186.15-3LNA SCO showed pronounced phosphorylation when activated with anti-IgM (Figure 5B). The level was almost as high as in WT cells, suggesting functional restoration of BTK.

B-PMOs efficiently promote splice correction in primary B cells. We next evaluated the effects of naked delivery into primary cells. The non-PMO SCOs, initially evaluated in the reporter gene assay (Supplemental Figure 2), were again selected based on potency and assessed in primary B cells. In contrast to the gymnotic effect seen in the reporter cell line, we were unable to detect any significant reproducible correction of the *BTK* mRNA in primary B cells under these conditions (data not shown). We subsequently evaluated the B-PMO 186.25 as well as the corresponding control, PMO 186.25. Notably, treatment with 3 μM B-PMO 186.25 produced corrected *BTK* mRNA (Figure 6A) as well as restored BTK protein expression (Figure 6B) in B cells from the BAC transgenic mice.

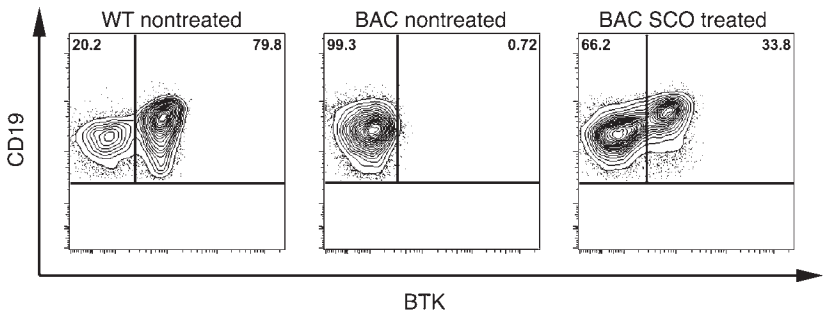

Figure 7. Restoration of BTK protein expression after splice correction in pro–B cells from BAC transgenic mice. Cells were electroporated with the 186.15-3LNA SCO. After 48 hours, cells were stained with anti-CD19 and anti-BTK (recognizing both mouse and human protein) for FACS analysis. Numbers in the 3 right upper quadrants indicate the percentage of CD19-positive and BTK-positive cells. The experiment was repeated twice with a similar outcome, and a representative result is presented.

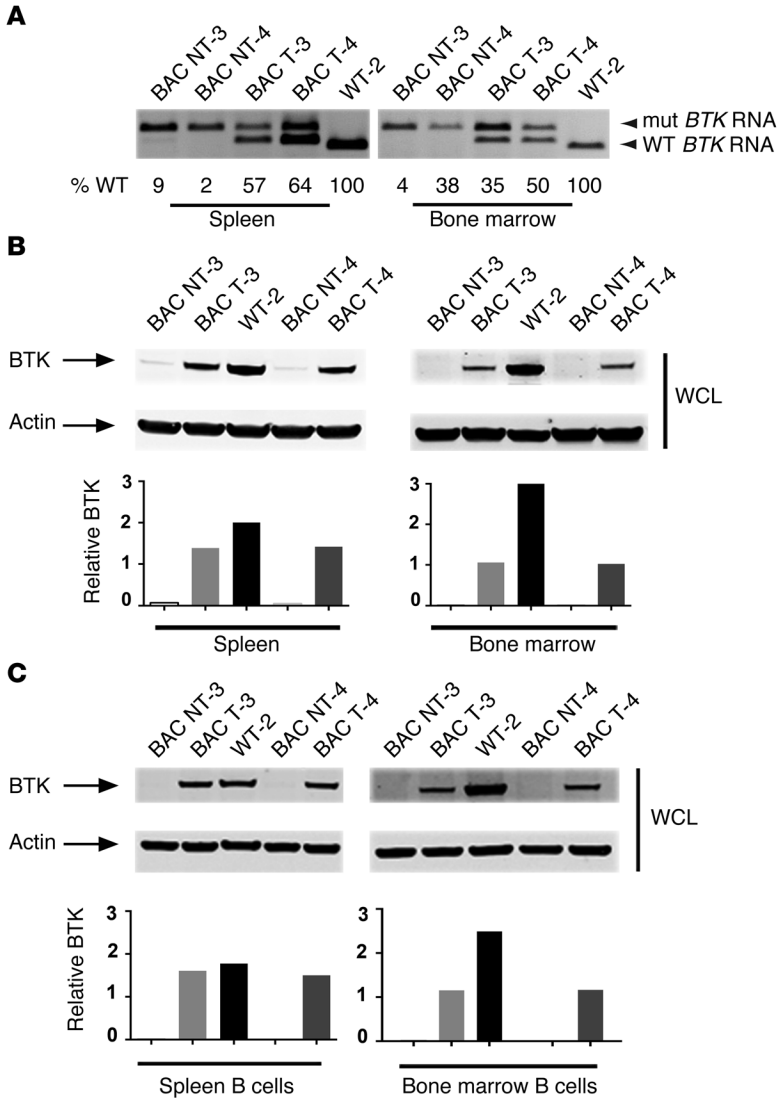

Figure 8. Restoration of BTK expression upon splice correction after in vivo treatment of BAC transgenic mice. Four mice were treated with B-PMOs, as described in Methods, and assayed for BTK restoration. (**A**) RT-PCR analysis of total spleen and total bone marrow cells from B-PMO–treated transgenic mice. A representative gel from 2 animals, both from the treated and the untreated group, is shown. "WT-2" represents RNA from normal mice, and the slightly smaller amplicon in this lane results from a differential primer set discriminating human and mouse RNA. To ascertain the detection of corrected transcripts for samples from treated and untreated BAC transgenic animals, we decided to use 3 times more cDNA and 5 more amplification cycles. (**B**) Western blot analysis of BTK restoration in 2 of 4 treated animals; total cells from bone marrow and spleen. (**C**) Western blot analysis of the isolated B cells both from spleens and bone marrow, showing BTK expression from 2 representative animals. The percentage of WT *BTK* RNA was calculated as WT RNA fraction × 100/(misspliced + WT RNA fraction). Bar graphs show the quantitative analysis of BTK protein as a percentage of relative intensity according to ImageJ Software. T, treated.

SCOs restore BTK protein expression in pro–B cells from the BAC transgenic mouse. Patients with XLA are devoid of mature B cells but harbor differentiation-arrested pro–B cells in their bone marrow (13, 60). Because of this fact, it was important to establish whether these cells are also amenable to SCO treatment as a proof of concept. For this reason, we first isolated and differentiated c-KIT$^+$ progenitor cells from the bone marrow of BAC transgenic mice. With support of OP9 stromal cells, Flk-2/Flt3 ligand, KIT ligand, and IL-7, the expansion of pro–B cells was induced in vitro (see Methods). After 9 days, an essentially pure pro–B cell population was obtained (Supplemental Figure 6). We subsequently transfected these cells with the 186.15-3LNA SCOs and assessed BTK protein expression at 48 hours. Encouragingly, as many as 33.8% of the pro–B cells were BTK positive (Figure 7).

In vivo administration of SCOs restores BTK expression in BAC transgenic mice. In order to investigate whether the SCOs also had the capacity to correct the defect in vivo, 4 animals were treated with a multiple-dose regimen using B-PMO 186.25. They received B-PMO 186.25 (30 mg/kg) 4 times: 3 doses intravenously every second day during 1 week, followed by a single subcutaneous dose; animals were assayed after another 3 or 4 days, respectively. As is depicted in Figure 8, A and B, and Supplemental Figure 7, a robust therapeutic effect was observed both in the bone marrow and in the spleen. In contrast to control mice, all treated mice expressed corrected *BTK* mRNA as well as BTK protein. Moreover, we isolated B cells from 2 treated and 2 untreated animals in order to be able to analyze BTK restoration specifically in this cell type. As shown in Figure 8C, we found that B-PMO was taken up by B cells both in bone marrow and spleen, as evidenced by the restored BTK expression.

Collectively, this suggests that the splice correction concept could become a viable treatment option for patients with XLA, although standardization of multiple parameters is needed prior to any clinical approach.

SCOs correct splicing and restore BTK protein in monocytes from patients with XLA ex vivo. As a final proof of concept in a human setting, we applied our strategy to primary patient cells. Similar to B cells, monocytes express the *BTK* gene but, in contrast, do not need BTK protein for normal development or survival (9, 13). Since patients with XLA essentially lack circulating B cells but do have normal numbers of circulating monocytes, we obtained monocytes from a patient with the *BTK* intron 4 cryptic splice site mutation. Since splicing factors in mice and humans are similar but not identical, it was important to ascertain that splice correction of full-length pre-mRNA also could take place in primary patient cells.

Electroporation conditions for transfection of SCOs into human monocytes were optimized, and their therapeutic effect was assessed. Using 186.15-3LNA, splice correction was observed for *BTK* both at the RNA (Figure 9A) and protein level (Figure 9B). Moreover, we also evaluated naked uptake of B-PMO 186.25 in patient monocytes, and SCOs readily restored *BTK* mRNA in these cells (Figure 9C) as well as yielded the corresponding protein dose dependently (Figure 9D). Even at a very high concentration (10 μM), PMO 186.25, devoid of the CPP moiety, did not restore BTK protein synthesis, suggesting the crucial importance of the CPP.

Thus, the results obtained in splice-corrected monocytes derived from a patient with XLA are in concordance with the

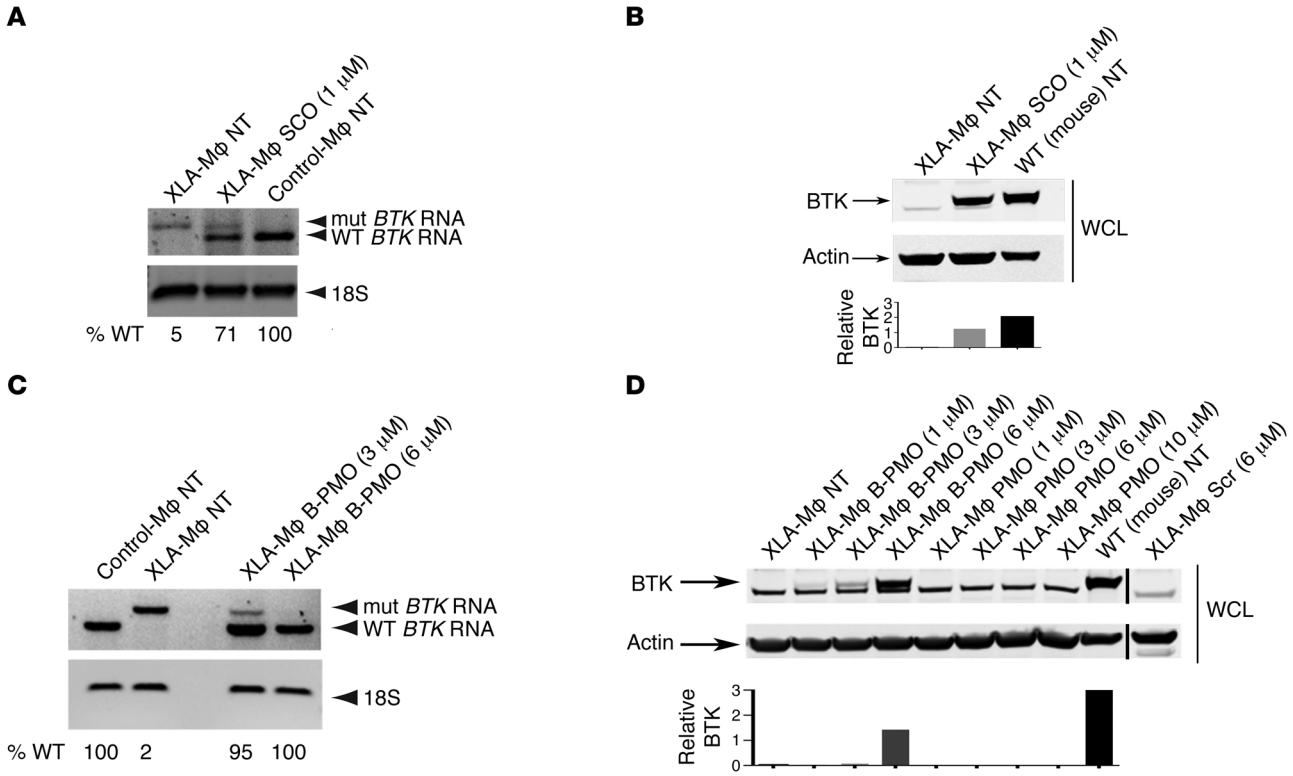

Figure 9. SCO-induced BTK restoration in patient monocytes. (**A**) Results from RT-PCR 48 hours after electroporation of monocytes from a patient with XLA with the intron 4 mutation. Monocytes were transfected with 1 μM 186.15-3LNA. Human control monocytes were also included. Ribosomal RNA (18S) serves as an RNA quality control. (**B**) Western blot showing BTK protein 48 hours after electroporation with or without treatment with 1 μM 186.15-3LNA. The right lane with a mouse B cell sample serves as a positive control for BTK (mouse and human BTK protein are both composed of 659 amino acids and recognized by the same antiserum). (**C**) RT-PCR results from patient monocytes treated with B-PMO 186.25 (3 μM and 6 μM). (**D**) Western blot showing BTK protein from B-PMO 186.25– and PMO 186.25–treated patient monocytes. Note that the anti-BTK antibody used for the monocyte lysates generates a strong, nonspecific band appearing just below the BTK-specific band, while the specific band is completely absent from the nontreated patient control cells (lane 1). Actin served as a loading control. Representative gels from 3 independent experiments are shown. The lanes separated by a black line were run on a different gel. The percentage of WT *BTK* RNA was calculated as WT RNA fraction × 100/(misspliced + WT RNA fraction). The bar graphs show the quantitative analysis of BTK protein as a percentage of relative intensity according to ImageJ Software. MΦ, monocytes.

findings in B lymphocytes from BAC transgenic mice both in vitro and in vivo. Collectively this demonstrates that splicing of full-length mutant human *BTK* pre-mRNA can be efficiently corrected by the SCOs, thereby suggesting that our strategy is viable in a human setting.

Discussion

In this report, we describe a novel BAC transgenic mouse model for human XLA and demonstrate its feasibility for the study of splice correction therapy. To the best of our knowledge, there is only a single existing human transgenic animal model for hematopoietic disease caused by aberrant splicing (61). The unique features of our transgenic mouse are that the entire affected locus is of human origin and that the corresponding endogenous gene has been deleted. This is also the first human transgene model for treatment strategies caused by defective splicing in the lymphoid compartment. Furthermore, owing to the fact that the BAC also encompasses the *HNRNPH2* splice-factor encoding gene, these mice express an additional component of human origin, making this model even more similar to the situation in XLA. Taken together, this suggests that our human BAC transgenic mouse could become of broad interest.

Mutations interfering with splicing events are estimated to account for a substantial amount of all alterations leading to disease (62), and XLA is no exception, with 14% of all mutations being caused by defects related to splicing (63, 64). In this study, we investigated a case of XLA caused by a single nucleotide replacement (A to T) in intron 4 of the *BTK* gene, which leads to aberrant splicing resulting in the inclusion of a cryptic exon containing an in-frame termination codon. The aim was to promote the exclusion of the erroneous exon and restore normal splicing in both patient with XLA and mouse model cells. Here, we have tested a number of ON chemistries and demonstrated their different properties and utility as therapeutics in leukocytes.

Design of efficient SCOs requires careful examination of both the *T*m and the uniqueness of the target sequence and, when possible, analysis of the secondary structure of the target site. Furthermore, the in vivo activity of any SCO is not only dependent on hybridization properties, but also on resistance to degradation and clearance as well as on uptake and intracellular release in the target cell. We initially tested a battery of 2′OMePS RNA ONs in a model cell line expressing an EGFP-luciferase fusion reporter gene interrupted by the *BTK* intron 4 with the same mutation as in the studied family with XLA. We scanned the whole exon 4a by designing differ-

ent SCOs primarily targeting ESE sites. Using the reporter cell line readout, we could observe robust splice correction, as evidenced by restored mRNA, thus confirming the potential of this approach, and the best-performing SCO candidates were selected for the next round of experiments. Of note here, SCOs complementary to the 3′ss of the cryptic exon showed lower efficiency compared with the other targeted sites. This might be due to the presence of secondary structures in the 3′ss, making the SCOs less efficient.

Studies in the cell line model allowed us to screen different LNA-modified versions of the SCOs to achieve further enhanced splice correction. Since LNA ONs are normally more potent, we investigated size-reduced versions. By decreasing the length from the initial 18-mers to 15-mers, the idea was that smaller SCOs could provide an advantage in terms of cellular uptake and release and hybridization specificity (49, 65). Thus, the efficiency of 2′OMePS SCOs was compared with the corresponding shorter versions. Hence, in comparison to an 18-mer 2′OMePS RNA, the various 15-mers composed of LNA/2′OMePS RNA had similar, or even higher, activity. The size factor is of relevance, since shorter ONs have reduced risk of accidentally targeting irrelevant RNA sequences if appropriately designed. The resulting enhanced target specificity can potentially allow lower doses to be administered while activity in vivo is maintained (34, 49, 53). However, we also observed that further shortening of the SCOs, as measured in this in vitro model, reduced the splice-correcting activity of both the 186 and the 187 series. This may be secondary to the fact that the avidity of very short ONs simply is too low or to the fact that short ONs are less likely to interfere with splicing.

Next, the activity of the SCOs was assessed in the context of full-length, mutated human *BTK* pre-mRNA using either cells derived from the human BAC transgenic mouse or from primary patient monocytes carrying the intron 4 mutation. Although not all SCOs with different chemistries and lengths were compared between these 2 readouts, those tested behaved similarly. Thus, there was no indication of any unique secondary pre-mRNA structures imposing an altered sensitivity to the SCO-induced correction. This suggests that the identified SCOs, at least from this perspective, could be applied in a clinical setting.

To the best of our knowledge, this is the first time that exon-skipping SCOs have been successfully attempted as a treatment in primary B lymphocytes, adding this lineage to the list of potential targets for such a therapeutic intervention (66). Of crucial importance was the fact that we had the chance to obtain primary monocytes from a patient with XLA and successfully treat them with SCOs. This further substantiates the therapeutic potential of our SCO-based approach.

To this end, we also wanted to study naked delivery to both primary B cells and patient monocytes. Recently, PMO-based SCOs have proven to be very efficient in DMD animal models, especially when conjugated to a short arginine-rich peptide (i.e., B-PMO) belonging to the CPP group (67). Moreover, a D–amino acid–containing CPP-PMO was used in a thalassemia transgenic mouse model (68). Thus, in the context of splice switching, several CPPs, including the B-PMO, have been used to enhance PMO delivery, allowing the dose to be reduced by 1 order of magnitude or more in vivo (33). Moreover, antisense PMOs (23) and, even more potently, when conjugated to the B-peptide, such SCOs were successfully used by Gatti and collaborators to treat lymphoblastoid cell lines derived from patients with ataxia telangiectasia (24). In the latter report, it was also demonstrated that fluorescently labeled CPP-PMOs could cross the blood-brain barrier.

While almost full restoration was obtained with B-PMO 186.25 in patient monocytes, the correction under gymnosis conditions was weaker in primary B cells as compared with that under electroporation. It should be noted that the restored mRNA, as expected, was more stable than the aberrantly spliced transcript. Here, it is likely that optimization of primary cell culture conditions enabling long-term survival would allow uptake over several days, which is necessary for optimal gymnosis (53). Besides, the phagocytic nature of monocytes might enable easier translocation of CPPs in a shorter time. Since there is frequently a high capacity in endogenous signal transduction pathways, with only a fraction of proteins being, for example, phosphorylated, it is possible that correction of every defective *BTK* pre-mRNA is not needed for a therapeutic effect. Our findings with CPP-conjugated SCOs are reminiscent of the results obtained in DMD mice (57, 69, 70), in which B-PMOs were extraordinarily active.

This is also the first time that such modified ONs have been proven to work ex vivo in primary lymphoid cells, suggesting that the B-PMO design could become a versatile combination chemistry not restricted to muscle cell delivery. Of note is the fact that we observed a decrease in cell viability with increasing B-PMO concentrations in B cells, whereas monocytes were more resistant. This may be due to the fragile nature of BTK-defective primary B cells compared with monocytes, which are not functionally affected by lack of this protein. Moreover, the fact that lymphoblastoid cell lines treated with B-PMO SCOs showed restoration of the ataxia telangiectasia protein for a period of 21 days following a single treatment (24) demonstrates that at least certain B-lineage cells are highly suitable targets.

Comparing delivery by electroporation in human monocytes and primary B cells, we observed that lower concentrations of LNA-containing SCOs (1 μM) were sufficient for the correction in monocytes. This could be attributed to the electroporation method itself, which monocytes are able to resist better, whereas B cells get more damaged. It is possible that the electroporation conditions per se reduced the actual number of lymphocytes that are both successfully transfected and surviving, which could result in an underestimation of the potency of the SCO after electroporation in B cells. On the other hand, there may be differences in the internalization of the SCOs and their subsequent intracellular routing. Moreover, the fact that primary human monocytes were readily transfectable also suggests that SCOs could represent a treatment option for monocyte disease.

Demonstrating not only protein restoration, but also the corresponding biological activity, was crucial for the splice-switch concept as a potential treatment modality. The fact that 2 different functional tests, cell viability and Y551 phosphorylation of BTK, yielded confirmatory results strongly suggests that the BTK protein generated is fully active.

Moreover, we also demonstrate that B-PMO 186.25 could be systemically administered in vivo, correcting the defect in mice lacking the endogenous protein but expressing the mutated human *BTK* gene. We could show that treated animals had substantial lev-

els of BTK expression both in the bone marrow and spleen, organs considered challenging for SCO therapy. Moreover, we could also demonstrate that isolated B cells, both from the bone marrow and spleen, expressed BTK, further proving that B-PMO reached the target cells and induced a therapeutic effect. At this stage, we have not made measurements allowing the detailed comparison between transcript and protein levels, for example, but rather, the analysis should be regarded as semiquantitative. The observation that upon treatment the relative amount of BTK in bone marrow cells seems to be lower is not unexpected, since it is likely that the splenocyte exposure to SCOs will be greater, due to the fact that more of the cardiac output reaches the spleen. One can also speculate that a fraction of BTK-expressing B-lineage cells in the bone marrow might constitute progenitor cells, adding a further therapeutic value. In this study, only a single multidose regimen was investigated, so it remains to titrate the dose and frequency of treatments to identify an optimal dosage. Importantly, treatment for just 1 week was sufficient for obtaining significant BTK restoration. Thus, it is quite possible that treatment periods longer than a week will further increase the number of corrected cells. The optimal mode of administration also remains to be tested. Since the treated mice were subject to combined intravenous and subcutaneous delivery, their respective contribution to the final treatment result cannot be estimated but deserves further studies.

Splenic B cells are easily accessible and constitute the preferred experimental source of mouse B cells. However, for obvious reasons, splenocytes are not the candidate target cells for SCO therapy in XLA and, instead, bone marrow–resident pro–B cells are. Therefore, we differentiated primary bone marrow progenitor cells into pro–B cells and subsequently transfected them with SCOs. Already after 48 hours, substantial amounts of BTK protein were detected in a high proportion of these cells, approximately to the same extent as that observed in mature B lymphocytes. This is an important piece of information, which suggests that the SCO treatment concept could become applicable in a patient setting. Furthermore, it is known that pro–B cells from human bone marrow can be expanded ex vivo as described before (71). It was gratifying to observe that in vivo administration of B-PMOs yielded BTK restoration not only in the spleen, but also in the bone marrow. This bodes well for the concept of correcting human pro–B cells.

We also investigated the possibility of using a dual approach, namely to complement the SCO therapy with treatment with antagomirs targeting miR-185, which has been reported to negatively regulate BTK expression in primary mouse cells (72). However, in preliminary experiments, the antagomir strategy was not sufficiently robust (unpublished observations). A single antagomir design was used in these experiments, and it may well be that further optimization could improve the outcome. Thus, combining different ON strategies remains an attractive option with recent success in experimental DMD (73).

A key feature of XLA is that BTK is expressed in all B-lineage stages, except for the mature plasma cell (8, 9). This opens the possibility that even a transient correction of B-lineage cells could result in a long-term treatment effect. Thus, if BTK expression could be transiently restored at the pro–B cell stage, yielding a polyclonal native B cell repertoire, such cells are expected to respond to immunization. Since infectious agents represent a major threat to patients with XLA, vaccination against them could potentially yield an adequate humoral immune response by SCO-corrected B cells. The primary B lymphocytes responding to the vaccine would subsequently maturate into BTK-independent long-lived plasma cells exerting long-term protection. Due to the fact that the B cell receptor is not expressed in plasma cells, this strategy is valid for all primary immunodeficiencies caused by splice site mutations affecting this receptor complex (1).

From a therapeutic point of view, it might be feasible to obtain pro–B cells, carry out the treatment ex vivo, and return the splice-corrected cells to the patient or, alternatively, to administer the SCOs systemically in vivo. Ex vivo treatment has the advantage that any potential side effect resulting from the uptake of SCOs in non–B-lineage cells could be avoided. On the other hand, such a treatment would be more cumbersome. Thus, in vivo administration might seem more straightforward, and even if the dosage has not been studied in detail, it is likely that rather large doses will be required. If such a medicine would become available, there would be additional aspects to take into consideration, e.g., the cost of synthesis, which is likely to be higher for in vivo delivery. Whether splice correction will ever become a treatment option for B cell disorders, or other hematopoietic diseases, remains to be seen. Here, we have developed a unique animal model allowing both ex vivo and in vivo research along this line to be conducted in a preclinical setting.

Methods

Design of SCOs. The bioinformatic algorithms of 3 different web-based splice servers, namely ESE Finder (74), PESX (75), and RESCUE-ESE (76), were used to aid in the design of the SCOs with the highest probability of success.

ONs. A list of the SCOs used is presented in Table 1. 2′OMePS RNA ONs were synthesized at GE Healthcare. LNA-containing ONs were synthesized at the University of Southern Denmark. PMO-based ONs were purchased from Gene Tools and conjugation to B-PMO made at the MRC Laboratory of Molecular Biology. ZEN-modified ONs were made by IDT.

Reporter plasmids. The pEGFPLuc plasmid (Clontech) was used to construct a reporter plasmid in which the luciferase cDNA was interrupted by the introduction of a mutated *BTK* intron 4 containing an A-to-T change known to result in aberrant splicing resulting in the inclusion of the cryptic exon (25). The introduction of this exon in the EGFP-luciferase fusion mRNA abolishes most of the luciferase activity. The final plasmid was designated pEGFPLuc/Btkint4mut. Cloning of the mutant *BTK* intron 4 into the EGFPLuc plasmid was done first by PCR amplification of a WT *BTK* gene intron 4, followed by site-specific mutagenesis to recreate the specific A-to-T change found in the patient. The cloning work was performed by Mutagenex Inc.

Cell culture and SCO transfections. The U2OS cell line stably expressing pEGFPLuc/Btkint4mut was generated by transfection of the plasmid with Fugene 6 (Roche) and selection of stable integrants for 3 weeks with 1 mg/ml Geneticin (Life Technologies). The stable cell line was designated U2OS/EGFPLucBTKint4mut. Cells were normally cultured in DMEM with 10% FBS and maintained at 37°C, 5% CO_2 atmosphere. For SCO transfections, cells were plated the day before at a density of 50,000 cells per well in a 24-well plate. Transfections were performed using Lipofectamine 2000 (Life Technologies) according to the manufacturer's protocol, and cells were further incubated for 24 hours. For the gymnosis/naked uptake experiments, cells were plated

to reach 70% confluency at the day of transfection. The cells were incubated further for 3 days with SCOs in DMEM containing 10% FBS.

Luciferase assay. For analysis of luciferase activity in the stably transfected U2OS cell line, cells were lysed in 300 μl RLT buffer (Promega), and 20 μl lysate was used for measuring luciferase activity with the Luciferase Assay Kit (Promega). Luminescence was detected using a FluoStar OPTIMA (BMG Labtech). Total protein was detected using the MicroBCA Kit (Pierce) and used for normalization of luminescence.

BAC constructs. A BAC construct carrying a mutated human *BTK* gene was obtained from TaconicArtemis GmbH. The mutated BTK construct was generated to contain a point mutation in intron 4 (A to T) at position 602 and sequence verified. This alteration is identical to that found in a Swedish family with XLA (25). The construct also contains genes and regulatory elements surrounding *BTK*, such as the genes *TIMM8A*, *RPL36A*, *GLA*, *HNRNPH2*, and part of *TAF7L*.

Generation and genotyping of BAC transgenic mice. Pronuclear injection of BAC DNA was performed at Karolinska Center for Transgene Technologies. Fertilized mouse oocytes were injected and later transferred into pseudo-pregnant females. The offspring were tested by DNA genotyping analysis. Ear or tail biopsies were collected from each mouse, and DNA was isolated (DNeasy Blood & Tissue Kit, Qiagen). PCR with HotStarTaq *Plus* DNA polymerase (Qiagen) was performed. Primers were designed to amplify human, but not mouse, *BTK* exons 1, 11, and 19 as well as *GLA* and *TAF7L* genes. Primer sequences were as follows: *BTK* exon 1 forward, 5′-agacattggtttaggtcagg-3′; *BTK* exon 1 reverse, 5′-ttttaggggtcccaagcaag-3′; *BTK* exon 11 forward, 5′-gagcaccacttcctcctaca-3′; *BTK* exon 11 reverse, 5′-gcacagcatcaaggagctat-3′; *BTK* exon 19 forward, 5′-cccttgaattctggattctag-3′; *BTK* exon 19 reverse, 5′-agcttgggatttcctctgaga-3′; *GLA* forward, 5′-gaatgccaaactaacagggc-3′; *GLA* reverse, 5′-caaagtgctgggattacagg-3′; *TAF7L* forward, 5′-caggtcacatgactacacagg-3′; and *TAF7L* reverse, 5′-gaaagaaggtcctcggctgg-3′. 5 μM of each primer was used. Cycling conditions were as follows: 95°C for 5 minutes, 30–35 cycles of 94°C for 30 seconds, 58°C (*BTK*) or 57°C (*GLA* and *TAF7L*) for 30 seconds, 72°C for 30 seconds, and a final incubation at 72°C for 10 minutes. RT-PCR analysis was also performed to assure the presence of human mutated *BTK* at the mRNA level in the founder animals. For this, RNA was isolated from purified B lymphocytes (EasySep Mouse B Cell Enrichment Kit, StemCell Technologies) using the RNeasy Plus Mini Kit (Qiagen). The RNA was reverse transcribed into cDNA using the First-Strand cDNA Synthesis Kit for RT-PCR (AMV) (Roche). Primer sequences were as follows: *BTK* intron 4 forward, 5′-cacacaggtgaactccagaaag-3′, and *BTK* intron 4 reverse, 5′-agagatactgcccatcgatccaga-3′. Cycling conditions were as follows: 95°C for 5 minutes, 30 cycles of 94°C for 30 seconds, 57°C for 30 seconds, 72°C for 30 seconds, and finally 72°C for 10 minutes. Suitable founder animals were selected for breeding and further experiments. Samples were run on 1.25% agarose gel and analyzed by Gel Doc system (Bio-Rad).

Genotyping of BAC transgenic mice bred on BTK KO background. Transgene-positive founder animals (C57BL/6 mice) were bred onto the BTK KO/C57BL/6 strain in order to create a human BAC transgenic mouse model expressing only the mutated human *BTK* gene. Here, a PCR was developed to distinguish among WT, heterogenic, and *Btk* KO mice. Primer sequences were as follows: *Btk* forward, 5′-ctgggaacttcctgacagag-3′, and *Btk* reverse, 5′-caaaagtgcctcaaatgtgg-3′. Cycling conditions were as follows: 95°C for 5 minutes, 40 cycles of 94°C for 30 seconds, 59°C for 30 seconds, 72°C for 2.5 minutes, and 72°C for 10 minutes. These primers detect exclusively mouse *Btk*.

Material from a patient with XLA. Monocytes from a patient with XLA with the above-mentioned A-to-T change in intron 4 of the *BTK* gene (25) were obtained by apheresis followed by elutriation performed at the Centre for Apheresis and Stem Cell Processing (CASH), Karolinska University Hospital. The obtained cells were ≥80% pure monocytes.

Mouse B lymphocyte preparation, culturing, and transfections. Purified splenic mouse B lymphocytes were obtained using an EasySep Mouse B Cell Enrichment Kit, which enriches cells through negative selection (StemCell Technologies). The purity of isolated B cells was checked by staining of the cell population with a PE-anti-mouse CD19 (BD Pharmingen), as analyzed by flow cytometry. Purity levels were always ≥90%.

After isolation, B cells were cultured in Iscove's Modified Dulbecco's Medium (IMDM) containing 15% FBS and 50 μM β-mercaptoethanol (Gibco, Life Technologies), with addition of 5 μg/ml CpG ON (obtained from DNA Technology A/S) for stimulation and improved survival of the cells in culture, as detailed in Hasan et al. (77). Lymphocytes were thus incubated with CpG ON for 3 to 4 hours before proceeding with the transfections.

Transfections were performed by electroporation using a Neon Electroporator (Invitrogen) and the 100 μl Tip Kit (Neon Transfection System, Life Technologies). The following settings were used: 2,100 V (pulse voltage); 20 ms (pulse width); 1 (pulse number). In brief, 2.4×10^6 cells per well were resuspended in T buffer, and a volume of no more than 10 μl SCO per transfection per tip (i.e., maximum SCO volume was never more than 10% of the total resuspension volume) was added to the resuspended cells. Nontreated samples were treated with 1× dPBS only. After the electrical pulse, the cells were transferred to a 24-well, nontissue culture-treated plate (Falcon, BD) with 400 μl IMDM medium containing 15% FBS and 50 μM β-mercaptoethanol. Cells were incubated for 4 hours, after which an additional volume of 500 μl medium was added together with 5 μg/ml CpG ON. Cells were subsequently incubated for 48 hours.

For the gymnosis/naked uptake experiments, cells were plated at 1.5×10^6 cells per well on the day of transfection. The same CpG treatment was done as described above. The SCOs were given directly to the cells. B-PMOs were incubated at 37°C for 30 minutes and sonicated for a few seconds in a water bath before use. The cells were incubated further for 3 to 4 days with SCOs.

XLA patient monocyte culturing and transfections. SCOs were transfected into the monocytes as described above with the following settings for the Neon Electroporator: 1,800 V (pulse voltage); 30 ms (pulse width); 1 (pulse number). After the electrical pulse, the cells were transferred to a 24-well, nontissue culture-treated plate (Falcon, BD) with 400 μl IMDM medium containing 15% FBS and 50 μM β-mercaptoethanol. Cells were incubated for 4 hours, after which an additional volume of 500 μl medium was added. Cells were further incubated for 48 hours. Gymnosis/naked uptake experiments were done as described in *Mouse B lymphocyte preparation, culturing, and transfections*.

Semiquantitative reverse transcription (RT-PCR). Cells stably transfected with the reporter gene (U2OS/EGFPLucBTKint4mut) were washed twice with 1xPBS, and RNA was directly isolated from the plated cells using the RNeasy Plus Kit (Qiagen). For the mouse B cells and human monocytes, cells were collected and centrifuged at 500 *g* for 5 minutes and washed in 1× Dulbecco's phosphate-buffered saline (dPBS; with no calcium and magnesium). RNA was isolated from the cell pellets using the RNeasy Plus Kit.

RNA was reverse transcribed into cDNA using the First Strand cDNA Synthesis Kit for RT-PCR (AMV-Roche). PCR was performed with HotStarTaq Plus DNA polymerase (Qiagen). An amount of 100 ng of total RNA was used. Primers for determining splice correction in the U2OS/EGFPLucBTKint4mut cells were as follows: *EGFPLuc* Fwd-5′-ctggtgccaaccctattctccttc; *EGFPLuc* Rev-5′-ccagatccacaaccttcgcttcaa-3′. The primers used in the case of human transgene, primary mouse B cells and human monocytes were as follows: *BTK* Fwd, 5′-cacacaggtgaactccagaaag, and *BTK* Rev, 5′-agagatactgcccatcgatccaga-3′. For the WT primary mouse B cells, another forward primer was used: *Btk* Fwd2, 5′-gagcatctttctgaagcgatccca-3′. Cycling conditions were as follows: 95°C for 5 minutes, 30 cycles of 94°C for 30 seconds, 57°C for 30 seconds, 72°C for 30 seconds, and finally 72°C for 10 minutes. As an RNA quality control 18S ribosomal RNA (18s rRNA) was also analyzed by PCR. The primer sequences were as follows: *18S* Fwd-5′ gtaacccgttgaaccccatt; *18S* Rev-5′-ccatccaatcggtagtagcg. Cycling conditions were as follows: 95°C for 5 minutes, 12 cycles of 94°C for 30 seconds, 57°C for 30 seconds, 72°C for 30 seconds, and finally 72°C for 10 minutes. Samples were run on 1.25% agarose gel and analyzed by Gel Doc system (Bio-Rad). In order to ascertain the detection of human *BTK* mRNA from in vivo treated and untreated samples, compared with all other experiments, we decided beforehand to use 3 times more cDNA and 5 extra amplification cycles. Gel densitometry analysis was done using QuantityOne Software (Bio-Rad) in order to calculate the percentage of WT RNA.

Immunoprecipitation and immunoblotting. Immunoprecipitation analysis was carried using Dynabeads protein G (Life Technologies) according to the manufacturer's protocol. Cell lysates were obtained, after washing cells in PBS twice, by incubation with lysis buffer (50 mM HEPES, pH 7.0, 120 mM NaCl, 10% glycerol, 1% NP-40, 0.5% sodium deoxycholate) supplemented with protease inhibitors (Complete Mini, Roche) for 30 minutes with repeated vortexing. Finally, the lysates were cleared by centrifugation. Proteins were separated on gradient 4%–12% SDS Bis-Tris NuPAGE gels (Life Technologies) and transferred onto nitrocellulose membranes using the Iblot system (Invitrogen). The membranes were then blocked with LI-COR Blocking Buffer (LI-COR Biosciences GmbH) and probed with specific primary antibodies. Western blots signals were scanned by using Odyssey Imager from LI-COR Biosciences GmbH. The following primary antibodies were used for detection: actin (A5441, Sigma-Aldrich), BTK (270-284, Sigma-Aldrich), phospho-BTK (pY551) (558129, BD), and BTK (611117, BD). The following secondary antibodies were used for detection: goat anti-mouse 800CW, goat anti-rabbit 800CW, goat anti-mouse 680LT, or goat anti-rabbit 680 (all from LI-COR Biosciences GmbH). Actin was used as loading control. Quantitative analysis of BTK protein was calculated as the percentage of relative intensity by ImageJ software according to the manufacturer's protocol.

Anti-IgM stimulation and functional assays. For the phosphorylation assay, 48 hours after electroporation, B lymphocytes were starved for 6 hours in IMDM without serum and CpG. Cells were then pelleted and resuspended in 5×10^6 cells per ml in 1x dPBS. Then anti-IgM was added to a concentration of 20 μg/ml, and cells were incubated for exactly 1 minute, as previously described (78). Cells were then harvested for immunoprecipitation and immunoblotting as described above.

For the viability test, 48 hours after electroporation, B lymphocytes were washed to remove the CpG and resuspended in complete medium with 2×10^6 cells per well. Subsequently, 20 μg/ml anti-IgM was added to stimulate the cells. The cells were further incubated for 24 and 48 hours. At each time point, the cells were counted using a Bürker chamber, and viability was determined by Trypan Blue (Invitrogen) exclusion. Goat $F(ab')_2$ anti-mouse IgM (1022-01, Southern-Biotech) was used for both assays.

Pro–B cell culture and expansion of c-KIT⁺ cells. Femurs were dissected from WT and BAC transgenic mice. Bone marrow was crushed in 5 ml 1x dPBS with 2% FCS and further subjected to magnetic-activated cell sorting column (Miltenyi Biotec) for enrichment of c-KIT⁺ cells. 10 μl immunomagnetic beads (Miltenyi Biotec) were used for the enrichment. After elution, the cells were resuspended in OPTIMEM (Life Technologies) containing 10% FCS, 50 μM β-mercaptoethanol, and 100X Penicillin-Streptomycin (Life Technologies). 10 ng/ml Flk-2/Flt3 ligand, 10 ng/ml IL-7, and 10 ng/ml KIT ligand (all from Peprotech) were added to the cell suspension. The cells were then put on top of a layer of OP9 cells seeded 1 day earlier, 11,000 cells per well in a 24-well plate, and incubated. OP9 cells were maintained in OPTIMEM with 10% FCS and 50 μM β-mercaptoethanol. At day 5, Flk-2/Flt3 ligand, IL-7, and KIT ligands were added again at the same concentration. Until day 9, the purity and the viability of the cells were checked daily by flow cytometry using CD19 and propidium iodide (Life Technologies). At day 9, the cells were 90% pure and used for the SCO treatment.

Flow cytometry. For the staining of B lymphocytes, cells were incubated in 1x dPBS with CD16/32 (clone 93, Biolegend) and subsequently incubated for 30 minutes at 4°C with CD19-PE (clone 1D3, BD). After washing twice with 1x dPBS, cells were resuspended in 1 μl/ml dPBS containing LIVE/DEAD Fixable Green Dead Cell Stain (Life Technologies) and further incubated for 30 minutes at 4°C. Then the cells were fixed using BD Cytofix/Cytoperm Kit according to manufacturer's protocol. Subsequently, cells were stained with BTK–Alexa Fluor 647 (clone 53/BTK, BD) and analyzed using a FACSCalibur instrument (BD) at the Center for Hematology and Regenerative Medicine, Karolinska Institutet.

For the analysis shown in Supplemental Figure 5, bone marrow cells were harvested, Fc blocked (CD16/32), and stained with the following combination of antibodies: LY6D-FITC (clone 49-H4, BD Bioscience), KIT-APC–Alexa Fluor 750 (2B8, eBioscience), B220-APC Cy7 (RA3-6B2, Bioscience), CD45.1-FITC (A20, eBioscience), CD25-PE (PC61, Biolegend), FLT3-PE (A2F10, eBioscience), CD19-PE-CF594 (1D3, BD), CD11c (N418, Biolegend), IgM-PE Cyanine 7 (11/41, eBioscience), Ly6c-APC (HK14, Biolegend), CD43-APC (S11, Biolegend), SCA1–Pacific Blue (D7, Biolegend), IgD–Pacific Blue (11-26c.2a, Biolegend), GRI-PE Cy5 (RB6-8C5, eBioscience), TER 119-PE Cy5 (TER119, eBioscience), CD3e- PE Cy5 (145-2c11, eBioscience), NK-1.1-PE Cy5 (PK136, Biolegend), Mac1-PE Cy5 (X), IL7Rbio (A7R34, Biolegend), and streptavidin-conjugated Qdot655 (Life Technologies) to visualize biotinylated antibodies as well as propidium iodine. For flow cytometry analysis, a LSR Fortessa instrument (BD) was used at the Center for Hematology and Regenerative Medicine, Karolinska Institutet. The analysis of the data was performed using the FlowJo Software.

BAC transgenic mice treated with B-PMO. Female age- and weight-matched BAC transgenic mice were used for the in vivo experiments. 200 μl B-PMO, freshly prepared as described above, or control vehicle (saline) was injected in the tail vein. The mice received 30 mg/kg B-PMO or saline every second day for 3 injections in total. After the last intravenous injection, the mice were injected subcutaneously with another 30 mg/kg B-PMO or saline to increase the time of circulating

B-PMO before harvesting of the organs. Two mice in each group on consecutive days were sacrificed 7 or 8 days after the first intravenous injection, and spleens and bone marrow were harvested for further analysis.

Statistics. Data are presented as mean ± SD. Statistical analysis was performed with Prism 6 (GraphPad Software). Statistical significance was determined using 1-way ANOVA, followed by Bonferroni's multiple-comparison test. $P \leq 0.05$ was considered statistically significant.

Study approval. All animal work was performed according to the protocols approved by the Ethical Committee on Animal Experiments, Stockholm South, Sweden. The animals were bred and maintained in accordance with Karolinska Institutet's guidelines for animal welfare. Patients provided informed consent, and research involving patient materials was approved by the regional ethical committee in Stockholm (20091309-31/2).

Acknowledgments

The project was supported by Swedish Research Council, Swedish County Council (ALF project), Swedish Cancer Society, and the Ragnar Söderberg Foundation. We would like to thank the people working in the animal facility at Karolinska Institutet; our special thanks to Maria Ottosson for the excellent help with the mouse breeding. We would like to thank A. Charlotta Asplund for performing mutation analysis of the *BTK* gene and Janne Turunen for critical reading of the manuscript. D.K. Mohammad holds a PhD fellowship from the Ministry of Higher Education and Scientific Research in the Kurdistan Regional Government (Erbil, Iraq). M.O. Gustafsson holds a PhD scholarship from Södertörn University College. The work in the laboratory of M.J. Gait was supported by the Medical Research Council (MRC programme no. U105178803).

Address correspondence to: C.I. Edvard Smith, Clinical Research Center, Department of Laboratory Medicine, Karolinska Institutet, Novum, Hälsovägen 7 SE-141 57 Huddinge, Sweden. Phone: 46.8.5858.3651; E-mail: edvard.smith@ki.se.

Amer F. Saleh's present address is: AstraZeneca R&D, Alderley Park, Safety Assessment UK, Cheshire, United Kingdom.

Tolga Sutlu's present address is: Nanotechnology Research and Application Center, Sabanci University, Istanbul, Turkey.

1. Berglof A, Turunen JJ, Gissberg O, Bestas B, Blomberg KE, Smith CI. Agammaglobulinemia: causative mutations and their implications for novel therapies. *Expert Rev Clin Immunol*. 2013;9(12):1205–1221.
2. Conley ME, et al. Primary B cell immunodeficiencies: comparisons and contrasts. *Annu Rev Immunol*. 2009;27:199–227.
3. Mohamed AJ, et al. Bruton's tyrosine kinase (Btk): function, regulation, and transformation with special emphasis on the PH domain. *Immunol Rev*. 2009;228(1):58–73.
4. Vetrie D, et al. The gene involved in X-linked agammaglobulinaemia is a member of the src family of protein-tyrosine kinases. *Nature*. 1993;361(6409):226–233.
5. Tsukada S, et al. Deficient expression of a B cell cytoplasmic tyrosine kinase in human X-linked agammaglobulinemia. *Cell*. 1993;72(2):279–290.
6. Vihinen M, et al. Mutations of the human BTK gene coding for bruton tyrosine kinase in X-linked agammaglobulinemia. *Hum Mutat*. 1999;13(4):280–285.
7. Smith CI, Islam TC, Mattsson PT, Mohamed AJ, Nore BF, Vihinen M. The Tec family of cytoplasmic tyrosine kinases: mammalian Btk, Bmx, Itk, Tec, Txk and homologs in other species. *Bioessays*. 2001;23(5):436–446.
8. de Weers M, et al. The Bruton's tyrosine kinase gene is expressed throughout B cell differentiation, from early precursor B cell stages preceding immunoglobulin gene rearrangement up to mature B cell stages. *Eur J Immunol*. 1993;23(12):3109–3114.
9. Smith CI, et al. Expression of Bruton's agammaglobulinemia tyrosine kinase gene, BTK, is selectively down-regulated in T lymphocytes and plasma cells. *J Immunol*. 1994;152(2):557–565.
10. Mangla A, et al. Pleiotropic consequences of Bruton tyrosine kinase deficiency in myeloid lineages lead to poor inflammatory responses. *Blood*. 2004;104(4):1191–1197.
11. Rawlings DJ. Bruton's tyrosine kinase controls a sustained calcium signal essential for B lineage development and function. *Clin Immunol*. 1999;91(3):243–253.
12. Khan WN. Regulation of B lymphocyte development and activation by Bruton's tyrosine kinase. *Immunol Res*. 2001;23(2–3):147–156.
13. Sideras P, Smith CI. Molecular and cellular aspects of X-linked agammaglobulinemia. *Adv Immunol*. 1995;59:135–223.
14. Lederman HM, Winkelstein JA. X-linked agammaglobulinemia: an analysis of 96 patients. *Medicine (Baltimore)*. 1985;64(3):145–156.
15. McKinney RE, Katz SL, Wilfert CM. Chronic enteroviral meningoencephalitis in agammaglobulinemic patients. *Rev Infect Dis*. 1987;9(2):334–356.
16. Ochs HD, Smith CI. X-linked agammaglobulinemia. A clinical and molecular analysis. *Medicine (Baltimore)*. 1996;75(6):287–299.
17. Gardulf A, Bjorvell H, Gustafson R, Hammarstrom L, Smith CI. The life situations of patients with primary antibody deficiency untreated or treated with subcutaneous gammaglobulin infusions. *Clin Exp Immunol*. 1993;92(2):200–204.
18. Winkelstein JA, Conley ME, James C, Howard V, Boyle J. Adults with X-linked agammaglobulinemia: impact of disease on daily lives, quality of life, educational and socioeconomic status, knowledge of inheritance, and reproductive attitudes. *Medicine (Baltimore)*. 2008;87(5):253–258.
19. Hermaszewski RA, Webster AD. Primary hypogammaglobulinaemia: a survey of clinical manifestations and complications. *Q J Med*. 1993;86(1):31–42.
20. Plebani A, et al. Clinical, immunological, and molecular analysis in a large cohort of patients with X-linked agammaglobulinemia: an Italian multicenter study. *Clin Immunol*. 2002;104(3):221–230.
21. Van der Hilst JC, Smits BW, van der Meer JW. Hypogammaglobulinaemia: cumulative experience in 49 patients in a tertiary care institution. *Neth J Med*. 2002;60(3):140–147.
22. Friedman KJ, Kole J, Cohn JA, Knowles MR, Silverman LM, Kole R. Correction of aberrant splicing of the cystic fibrosis transmembrane conductance regulator (CFTR) gene by antisense oligonucleotides. *J Biol Chem*. 1999;274(51):36193–36199.
23. Du L, Pollard JM, Gatti RA. Correction of prototypic ATM splicing mutations and aberrant ATM function with antisense morpholino oligonucleotides. *Proc Natl Acad Sci U S A*. 2007;104(14):6007–6012.
24. Du L, et al. Arginine-rich cell-penetrating peptide dramatically enhances AMO-mediated ATM aberrant splicing correction and enables delivery to brain and cerebellum. *Hum Mol Genet*. 2011;20(16):3151–3160.
25. Jin H, et al. Identification of Btk mutations in 20 unrelated patients with X-linked agammaglobulinaemia (XLA). *Hum Mol Genet*. 1995; 4(4):693–700.
26. Kralovicova J, Hwang G, Asplund AC, Churbanov A, Smith CI, Vorechovsky I. Compensatory signals associated with the activation of human GC 5' splice sites. *Nucleic Acids Res*. 2011;39(16):7077–7091.
27. Kole R, Krainer AR, Altman S. RNA therapeutics: beyond RNA interference and antisense oligonucleotides. *Nat Rev Drug Discov*. 2012;11(2):125–140.
28. Spitali P, Aartsma-Rus A. Splice modulating therapies for human disease. *Cell*. 2012;148(6):1085–1088.
29. Wang Z, Burge CB. Splicing regulation: from a parts list of regulatory elements to an integrated splicing code. *RNA*. 2008;14(5):802–813.
30. Hua Y, Vickers TA, Baker BF, Bennett CF, Krainer AR. Enhancement of SMN2 exon 7 inclusion by antisense oligonucleotides targeting the exon. *PLoS Biol*. 2007;5(4):e73.
31. Aartsma-Rus A, Janson AA, Heemskerk JA, De Winter CL, Van Ommen GJ, Van Deutekom JC.

Therapeutic modulation of DMD splicing by blocking exonic splicing enhancer sites with antisense oligonucleotides. *Ann N Y Acad Sci*. 2006;1082:74–76.
32. Koo T, Wood MJ. Clinical trials using antisense oligonucleotides in duchenne muscular dystrophy. *Hum Gene Ther*. 2013;24(5):479–488.
33. El Andaloussi SA, Hammond SM, Mager I, Wood MJ. Use of cell-penetrating-peptides in oligonucleotide splice switching therapy. *Curr Gene Ther*. 2012;12(3):161–178.
34. Lundin KE, et al. Biological activity and biotechnological aspects of locked nucleic acids. *Adv Genet*. 2013;82:47–107.
35. Veedu RN, Wengel J. Locked nucleic acids: promising nucleic acid analogs for therapeutic applications. *Chem Biodivers*. 2010;7(3):536–542.
36. Kaur H, Babu BR, Maiti S. Perspectives on chemistry and therapeutic applications of Locked Nucleic Acid (LNA). *Chem Rev*. 2007;107(11):4672–4697.
37. Lennox KA, Owczarzy R, Thomas DM, Walder JA, Behlke MA. Improved performance of anti-miRNA oligonucleotides using a novel non-nucleotide modifier. *Mol Ther Nucleic Acids*. 2013;2:e117.
38. Aartsma-Rus A. Overview on AON design. *Methods Mol Biol*. 2012;867:117–129.
39. Kang SH, Cho MJ, Kole R. Up-regulation of luciferase gene expression with antisense oligonucleotides: implications and applications in functional assay development. *Biochemistry (Mosc)*. 1998;37(18):6235–6239.
40. Roberts J, Palma E, Sazani P, Orum H, Cho M, Kole R. Efficient and persistent splice switching by systemically delivered LNA oligonucleotides in mice. *Mol Ther*. 2006;14(4):471–475.
41. Graziewicz MA, et al. An endogenous TNF-alpha antagonist induced by splice-switching oligonucleotides reduces inflammation in hepatitis and arthritis mouse models. *Mol Ther*. 2008;16(7):1316–1322.
42. Wahlestedt C, et al. Potent and nontoxic antisense oligonucleotides containing locked nucleic acids. *Proc Natl Acad Sci U S A*. 2000;97(10):5633–5638.
43. Graham MJ, et al. Antisense inhibition of proprotein convertase subtilisin/kexin type 9 reduces serum LDL in hyperlipidemic mice. *J Lipid Res*. 2007;48(4):763–767.
44. Lindholm MW, et al. PCSK9 LNA antisense oligonucleotides induce sustained reduction of LDL cholesterol in nonhuman primates. *Mol Ther*. 2012;20(2):376–381.
45. Guterstam P, et al. Splice-switching efficiency and specificity for oligonucleotides with locked nucleic acid monomers. *Biochem J*. 2008;412(2):307–313.
46. Arzumanov A, Walsh AP, Rajwanshi VK, Kumar R, Wengel J, Gait MJ. Inhibition of HIV-1 Tat-dependent trans activation by steric block chimeric 2′-O-methyl/LNA oligoribonucleotides. *Biochemistry*. 2001;40(48):14645–14654.
47. Fabani MM, Gait MJ. miR-122 targeting with LNA/2′-O-methyl oligonucleotide mixmers, peptide nucleic acids (PNA), and PNA-peptide conjugates. *RNA*. 2008;14(2):336–346.
48. Mizrahi RA, Schirle NT, Beal PA. Potent and selective inhibition of A-to-I RNA editing with 2′-O-methyl/locked nucleic acid-containing antisense oligoribonucleotides. *ACS Chem Biol*. 2013;8(4):832–839.
49. Straarup EM, et al. Short locked nucleic acid antisense oligonucleotides potently reduce apolipoprotein B mRNA and serum cholesterol in mice and non-human primates. *Nucleic Acids Res*. 2010;38(20):7100–7111.
50. Yeakley JM, Morfin JP, Rosenfeld MG, Fu XD. A complex of nuclear proteins mediates SR protein binding to a purine-rich splicing enhancer. *Proc Natl Acad Sci U S A*. 1996;93(15):7582–7587.
51. Johannsen MW, Crispino L, Wamberg MC, Kalra N, Wengel J. Amino acids attached to 2′-amino-LNA: synthesis and excellent duplex stability. *Org Biomol Chem*. 2011;9(1):243–252.
52. Campbell MA, Wengel J. Locked vs. unlocked nucleic acids (LNA vs. UNA): contrasting structures work towards common therapeutic goals. *Chem Soc Rev*. 2011;40(12):5680–5689.
53. Stein CA, et al. Efficient gene silencing by delivery of locked nucleic acid antisense oligonucleotides, unassisted by transfection reagents. *Nucleic Acids Res*. 2010;38(1):e3.
54. Stirchak EP, Summerton JE, Weller DD. Uncharged stereoregular nucleic acid analogs: 2. Morpholino nucleoside oligomers with carbamate internucleoside linkages. *Nucleic Acids Res*. 1989;17(15):6129–6141.
55. Summerton J. Morpholino antisense oligomers: the case for an RNase H-independent structural type. *Biochim Biophys Acta*. 1999;1489(1):141–158.
56. Popplewell LJ, Trollet C, Dickson G, Graham IR. Design of phosphorodiamidate morpholino oligomers (PMOs) for the induction of exon skipping of the human DMD gene. *Mol Ther*. 2009;17(3):554–561.
57. Yin H, et al. Cell-penetrating peptide-conjugated antisense oligonucleotides restore systemic muscle and cardiac dystrophin expression and function. *Hum Mol Genet*. 2008;17(24):3909–3918.
58. Khan WN, et al. Defective B cell development and function in Btk-deficient mice. *Immunity*. 1995;3(3):283–299.
59. Ellmeier W, et al. Severe B cell deficiency in mice lacking the tec kinase family members Tec and Btk. *J Exp Med*. 2000;192(11):1611–1624.
60. Noordzij JG, et al. Composition of precursor B-cell compartment in bone marrow from patients with X-linked agammaglobulinemia compared with healthy children. *Pediatr Res*. 2002;51(2):159–168.
61. Lewis J, et al. A common human beta globin splicing mutation modeled in mice. *Blood*. 1998;91(6):2152–2156.
62. Lopez-Bigas N, Audit B, Ouzounis C, Parra G, Guigo R. Are splicing mutations the most frequent cause of hereditary disease? *FEBS Lett*. 2005;579(9):1900–1903.
63. Holinski-Feder E, et al. Mutation screening of the BTK gene in 56 families with X-linked agammaglobulinemia (XLA): 47 unique mutations without correlation to clinical course. *Pediatrics*. 1998;101(2):276–284.
64. Valiaho J, Smith CI, Vihinen M. BTKbase: the mutation database for X-linked agammaglobulinemia. *Hum Mutat*. 2006;27(12):1209–1217.
65. Elayadi AN, Braasch DA, Corey DR. Implications of high-affinity hybridization by locked nucleic acid oligomers for inhibition of human telomerase. *Biochemistry*. 2002; 41(31):9973–9981.
66. Mourich DV, Iversen PL. Splicing in the immune system: potential targets for therapeutic intervention by antisense-mediated alternative splicing. *Curr Opin Mol Ther*. 2009;11(2):124–132.
67. Jearawiriyapaisarn N, et al. Sustained dystrophin expression induced by peptide-conjugated morpholino oligomers in the muscles of mdx mice. *Mol Ther*. 2008;16(9):1624–1629.
68. Svasti S, et al. RNA repair restores hemoglobin expression in IVS2-654 thalassemic mice. *Proc Natl Acad Sci U S A*. 2009;106(4):1205–1210.
69. Jearawiriyapaisarn N, Moulton HM, Sazani P, Kole R, Willis MS. Long-term improvement in mdx cardiomyopathy after therapy with peptide-conjugated morpholino oligomers. *Cardiovasc Res*. 2010;85(3):444–453.
70. Wu B, et al. Effective rescue of dystrophin improves cardiac function in dystrophin-deficient mice by a modified morpholino oligomer. *Proc Natl Acad Sci U S A*. 2008;105(39):14814–14819.
71. Kohn LA, et al. Lymphoid priming in human bone marrow begins before expression of CD10 with upregulation of L-selectin. *Nat Immunol*. 2012;13(10):963–971.
72. Belver L, de Yebenes VG, Ramiro AR. MicroRNAs prevent the generation of autoreactive antibodies. *Immunity*. 2010;33(5):713–722.
73. Cacchiarelli D, et al. miR-31 modulates dystrophin expression: new implications for Duchenne muscular dystrophy therapy. *EMBO Rep*. 2011;12(2):136–141.
74. Cartegni L, Wang J, Zhu Z, Zhang MQ, Krainer AR. ESEfinder: A web resource to identify exonic splicing enhancers. *Nucleic Acids Res*. 2003;31(13):3568–3571.
75. Zhang XH, Chasin LA. Computational definition of sequence motifs governing constitutive exon splicing. *Genes Dev*. 2004;18(11):1241–1250.
76. Fairbrother WG, Yeh RF, Sharp PA, Burge CB. Predictive identification of exonic splicing enhancers in human genes. *Science*. 2002;297(5583):1007–1013.
77. Hasan M, et al. Defective Toll-like receptor 9-mediated cytokine production in B cells from Bruton's tyrosine kinase-deficient mice. *Immunology*. 2008;123(2):239–249.
78. Mohammad DK, Nore BF, Hussain A, Gustafsson MO, Mohamed AJ, Smith CI. Dual phosphorylation of Btk by Akt/protein kinase b provides docking for 14-3-3zeta, regulates shuttling, and attenuates both tonic and induced signaling in B cells. *Mol Cell Biol*. 2013;33(16):3214–3226.